UNIVERSIDADE D
COIMBRA

MANOJ RAJANKUNTE MAHADESHWARA

STUDY OF THE TRIBOLOGICAL BEHAVIOR OF THE TEXTURED STEEL COATED WITH TMD FILMS

VOLUME 1

Dissertation under the Joint European Master's Degree in Surface Tribology and Interfaces guided by Prof Albano Cavaleiro and Dr Pooja Sharma presented to the Department of Mechanical Engineering of the Faculty of Science and Technology of the University of Coimbra.

July 2022

1 2 9 0

FACULDADE DE CIÊNCIAS E TECNOLOGIA
UNIVERSIDADE D COIMBRA

Study of the tribological behavior of the textured steel coated with TMD films

Submitted in Partial Fulfilment of the Requirements for the Degree of European Joint European Master in Tribology of Surfaces and Interfaces.

Estudo do comportamento tribológico do aço texturado revestido com filmes TMD

Author

Manoj Rajankunte Mahadeshwara

Advisor[s]

Prof. Albano Cavaleiro

Dr. Pooja Sharma

Jury

President	**Professor Doutor Bruno Trindade**
	Professor at Universidade de Coimbra
Vowel	**Professor Doutor Paula Piedade**
	Professor at Universidade de Coimbra
Advisor	**Doutor Pooja Sharma**
	Post doctoral Researcher at Universidade de Coimbra

· U C ·

UNIVERSIDADE DE COIMBRA

tribos Joint European Master in Tribology of Surfaces and Interfaces

Ljubljana • Leeds • Coimbra • Luleå

Coimbra, July, 2022

ACKNOWLEDGEMENTS

*I would like to recognize all the great support of my supervisors **Prof. Albano Cavaleiro** and **Dr. Pooja Sharma** for always guiding me and for contributing with new ideas to overcome the inherent obstacles of scientific investigation. Additionally, I would also like to acknowledge the help and suggestions provided by **Dr. Amilcar Ramalho**, **Dr. Luis Vilhena**, **Dr. Todor Vuchkov**, **Eng. Fatima Rosa**, and the technical staff of **IPN**, who have contributed to this research with their experience. I would also like to acknowledge the project **Atrito-0**, as this study is part of that project as well as **Vipin Richhariya** and **MAHLE** industry for helping in texturing process.*

*I would also like to express my sincere appreciation to all the knowledgeable Professors, lecturers, and Colleagues from the University of Leeds, Ljubljana, and Coimbra for all the guidance and support that I received in these two years, helping with the completion of this master's program. Many thanks to **TRIBOS Consortium** and my **TRIBOS** mentors **Prof. Ardian Morina, Prof. Mitjan Kalin and Prof. Bruno Trindade** for their support and selecting me for this prestigious program.*

Finally, I thank my family for continually motivating and supporting me throughout this journey. Above all, to the great Almighty God, who is the creator of this universe and beyond.

Abstract

Surface texturing is one of the techniques which is widely used on various machine components such as piston/cylinders to prevent their early breakage and increase their functionality. The texture on the surface aids the lubrication and reduces the coefficient of friction (COF) and wear. The functioning of the texture on the surface is varied by various parameters such as the method of texturing, shape of texture, operating conditions etc. Similarly, surface coating is also another technique for enhancing the surface properties of the materials. Surface coating acts as a solid lubricant on the surface in case of wear and tear and reduces COF. Since enhancing the tribological properties of the piston/cylinder materials in an internal combustion engine is important to benefit the fuel economy and performance of the engine. Proper lubrication in these systems is a key feature which can improve their tribological performance. The objective of this work is the significant reduction in friction in different lubricated regimes in particular boundary lubrication (BL), mixed lubrication (ML) and hydrodynamic lubrication (HL) regimes. The novel solid lubricant coatings combined with surface texturing can decrease the friction without harming environment with oil additives. The synergetic effect of transition metal dichalcogenides (TMD) coatings applied onto textured surfaces can help to achieve this goal. Texturing procedure will consist in 2 steps: (i) texturing of electrodes using laser technology with three different geometric patterns (two rectangular and one circular) and (ii) texturing of specimens by ECP (electrochemical processing) / EDM (electric discharge machining) using these textured electrodes. The texturing techniques used in this investigation are ECP and dual texturing with EDM+ECP in combination with TMD coatings (WSC and MoSeC) via physical vapor deposition (PVD). The effect of these three texture geometries and TMD-based coatings were analyzed with block-on-ring tribological test to see the effect of different textures, texturing processes, coatings and combined effect of texturing and coatings. The biggest improvement in terms of COF reduction for textured-coated specimen was observed in circular dimpled specimen in BL regime at low sliding speeds and in ML and HL regime at high sliding speeds.

Keywords: Surface texturing, ECP/EDM texturing, TMD coatings, Block-on-ring, Stribeck curve

Resumo

A texturização de superfície é uma das técnicas amplamente utilizadas em vários componentes de máquinas, como pistão/cilindros, de modo a evitar sua quebra precoce e aumentar sua funcionalidade. A textura na superfície auxilia na lubrificação e reduz o coeficiente de atrito (COF) e o desgaste. O funcionamento da textura na superfície depende de vários parâmetros, como o método de texturização, a forma da textura, condições de operação, etc. Da mesma forma, o revestimento da superfície também é outra técnica usada para melhorar as propriedades da superfície dos materiais. O revestimento de uma superfície atua como um lubrificante sólido na mesma em caso de desgaste e reduz o COF. Uma vez que o aprimoramento das propriedades tribológicas dos materiais pistão/cilindro num motor de combustão interna é importante para beneficiar a economia de combustível e o desempenho do motor. A lubrificação adequada nesses sistemas é, assim, uma característica fundamental que pode melhorar seu desempenho tribológico. O objetivo deste trabalho consiste na redução significativa do atrito em diferentes regimes de lubrificação, em particular, em regimes de lubrificação limite (BL), lubrificação mista (ML) e lubrificação hidrodinâmica (HL). Os novos revestimentos de lubrificantes sólidos combinados com a texturização da superfície podem diminuir o atrito sem prejudicar o meio ambiente com aditivos de óleo. O efeito sinérgico dos revestimentos de dichalcogenetos de metais de transição (TMD) aplicados em superfícies texturizadas pode ajudar a atingir esse objetivo. O procedimento de texturização consistirá em duas etapas: (i) texturização de elétrodos, utilizando tecnologia laser com três padrões geométricos diferentes (dois retangulares e uma circular) e (ii) texturização de corpos de prova por ECP (processamento eletroquímico) / EDM (usinagem por descarga elétrica) utilizando esses elétrodos texturizados. As técnicas de texturização utilizadas nesta investigação são ECP e a texturização dupla com EDM+ECP em combinação com revestimentos TMD (WSC e MoSeC) por deposição física de vapor (PVD). O efeito destas três geometrias de textura e dos revestimentos baseados em TMD foram analisados com teste tribológico de bloco sobre anel para ver o efeito das diferentes texturas, dos processos de texturização, revestimentos e o efeito combinado de texturização com os revestimentos. A maior melhoria em termos de redução de COF para corpos de prova

texturizados, foi observada em amostras de covas circulares em regime BL com baixas velocidades de deslizamento e em regime ML e HL a altas velocidades de deslizamento.

Palavras-chave: Texturização de superfície, Texturização ECP/EDM, Revestimentos TMD, Block-on-ring, Curva Stribeck

CONTENTS

[LIST OF FIGURES]

[LIST OF TABLES]

[ACRONYMS/ABBREVIATIONS]

3D- Three-dimensional

BL - Boundary lubrication

COF - Coefficient of friction

ECP - Electrochemical processing

ED - Electric discharge

EDM - Electric discharge machining

HL - Hydrodynamic lubrication

BL – Boundary lubrication

IPN - Instituto Pedro Nunes

LST - Laser surface texturing

ML - Mixed lubrication

PVD - Physical vapor deposition

SEM - Scanning electron microscopy

EDS - Energy dispersive X-ray spectroscopy

WSC - Tungsten-sulfur-carbon

BSE - Back scattered electrons

MoSeC – Molybdenum-selenium-carbon

CHAPTER 1

1. INTRODUCTION

The present research work entitled 'Study of the tribological behavior of the textured steel coated with TMD films' emphasis on the effect of different surface texturing techniques (ECP, EDM, dual texturing), texture geometries and surface coatings (WSC, MoSeC) on the tribological behavior of the steel specimens. This study compares the contribution of the above-mentioned textured techniques and coatings in improving the frictional properties of the specimens. It will help to determine the best suited texturing technique, geometry and coating for the piston/cylinder surface enhancement applications. It will be interesting to analyze how synergy of texturing and post coating will makes difference in overall performance of specimen in different lubrication regimes.

The increasing demand for the high performance of the engine with low energy consumption has raised the concerns of controlling the friction and wear behaviors of the materials. Enormous studies have been conducted in the last few decades to solve the problems concerning to the tribological aspects of the piston/cylinder components [1- 4]. Different solutions have been identified by the scientific community; one such solution for improving the tribological characteristics of the mechanical components is surface texturing. Surface texturing acts like lubricant reservoir and helps in reducing the friction and wear rate of the components [5]. There are different types of surface texturing techniques namely EDM, laser surface texturing (LST), ECP, shot blasting, micro grinding, focused ion beam machining etc. that have been recorded in the literature [6]. Each technique is different from one another and has its own advantages and disadvantages with respect to accuracy, flexibility, cost of fabrication etc. Hence the texturing technique can be based on the required application. [7]. However, the eventual goal of every technique is to enhance the tribological properties in the components for the given application. Various theoretical and experimental researches [12-16] on surface texturing for tailoring the properties of steel have been stated that the surface texturing helps in reducing the friction and wear. Based on these research works, the surface texturing techniques were implemented in various applications, such as cutting tools [8], mechanical seals [9], piston/cylinders [10], bearings [11] and prosthetic joints [12]. Surface texturing via different techniques results in diverse surface morphology

that modifies the frictional performance of the textured surface. However, there are few reports documented in literature based on effect of different texture patterns (shape and size) on the tribological properties [13]. These studies arises a keen interest in the researchers for exploring better technique to acquire the required texture patterns.

Another method reported in literature for surface modification is the surface coating; this technique helps in self-lubrication on the material surface in the course of machining operation [14]. It acts as a solid lubricant on the surface and reduces the COF and wear to improve the tribological properties [15]. Various coating techniques such as PVD, chemical vapor deposition, galvanizing etc. are used to deposit different type of coatings on the specimen [16].

The selection of the surface texturing technique and coated material completely depends on the requirements and specifications of the application they are going to be used. Since, TMD coatings are well researched for its self-lubricating properties so implementation of TMD coatings on the textured surface would further results in enhancing the surface tribological properties.

In the present study, different texture geometries textured by ECP on steel specimens have been studied before and after coating to optimize the best performing pattern. Further, the best performing pattern (circular pattern) has been textured with dual texturing method and analyzed to observe the impact of texturing techniques. Along with it, two types of coatings MoSeC and WSC coatings have been studied on smooth and textured specimens. This study explores the effect of combination of the surface texturing and coating on the tribological behavior in different lubrication regimes and lead to the results that are different when studied individually.

1.1. Motivation

Surface texturing and surface coating elevates tribological characteristics of piston/cylinder materials by improving the lubrication performance. Texturing provides the storage of extra oil acting as lubricant reservoir and coating provides solid lubrication that helps in lowering the COF and wear. Hence, surface texturing results in modification of surface morphology altering its frictional performance in ML and HL region and surface coating is helpful in providing solid lubricant in BL regime. Various theoretical and

experimental researches on surface texturing and coating have been investigated for tailoring the properties of steel. These studies raise a keen interest to observe the synergetic effect of TMD coatings applied onto textured surfaces. The effect of this combination; surface texturing and coating can be helpful in overall improvement of the COF in all three regimes.

1.2. Thesis Organization

This thesis entitled "Study of the tribological behavior of the textured steel coated with TMD films" has been divided into five chapters. Chapter 1 introduces to the understanding of surface texturing and surface coating techniques and the combined study contributing to the field of tribology. Chapter 2 presents a concise review of the literature on surface texturing techniques, texture geometries and their influence on tribological behavior, surface coating techniques and different TMD coatings etc. Chapter 3 provides detailed description about the experimental methods; this includes description about the electrodes and specimens used for the current research, details of various experimental techniques, experimental conditions employed and parameters fixed for individual experimentation. Chapter 4 includes the characterizations of the electrodes and specimens before and after tribological tests and describes results and discussions of completed tribological experiments. Chapter 5 includes final conclusions of the thesis with recommendations for future work.

CHAPTER 2

2. STATE OF ART

This project investigates the effect of the surface texturing and surface coating techniques on tribological properties of steel. In this chapter the previous research related to the topic of interest is summarized. This covers from the basic definitions of the surface texturing and coating methods, working principle and the summary of the research findings of the previous research based on various applications.

2.1. Surface Texturing

The concept of using the surface texturing to reduce friction at the contacts was used in 1966 by Hamilton et al., [17] However this technique is a contrary to the belief of smooth surfaces to reduce friction [18]. Surface texturing has played an important role in the cutting tool application by preventing the premature failure of the tool. The tool life is one of the most important aspects considered during the designing of the cutting tool. In order to reduce the friction and wear in the cutting tools, the cutting fluids are most commonly used that acts as a lubricant and cooling agent. [19] However their function is only prominent at low cutting speeds and in case of the high cutting speeds, due to the shortage in the time for the cooling action the cutting fluids would not be able to function in the tool-workpiece interface. Also various other methods such as high-pressure water jet technique etc are used as the cooling techniques however, these techniques contributes only in the heat reduction and not in reducing the friction and wear. Hence surface texturing technique plays an important role in cutting tools that acts like a cooling agent and contribute in reducing the friction and wear. [20]

Surface texturing is defined as the process of generating the specific type of the pattern on the given surface in order to change its surface properties [21]. The term ‘texturing’ is defined as the engineered surfaces which contains the multiple features consisting of micro holes, micro asperities, dimples or micro/nano patterns at multiple levels of exact geometric parameters, these are purposely manufactured in order to enhance the functionality of the

given surfaces [21]. The application of surface texturing technique can be observed in the nature, the presence of the 3-dimensional rib pattern on the shark skin that helps in reducing the drag as well as reduction in turbulent wall shear is one example [22]. The hydrophobicity in the leaves of lotus plant helps as water repellant flooring which is a type of micro pillar array texture [23]. The surface roughness parameter is one of the important parameters in the hip implant of the human body because; the cell attachment and human fibroblast growth on the surface can be regulated by changing the surface contact angle of the implant [24]. The machines undergoing high frictions such as the piston ring and thrust bearings are implemented with the texturing techniques like LST and ECP. The micro dimples created on these machines reported the decrease in friction and increase in seal life [25]. The surface texturing in the field of aerodynamics and hydrodynamics is very important to reduce the fluid drag. The transparent plastic film with surface texture was employed on the aircraft in the direction of the air flow. This reduced the aircraft drag up to 8% resulting in reducing the fuel consumption up to 1.5% [26].

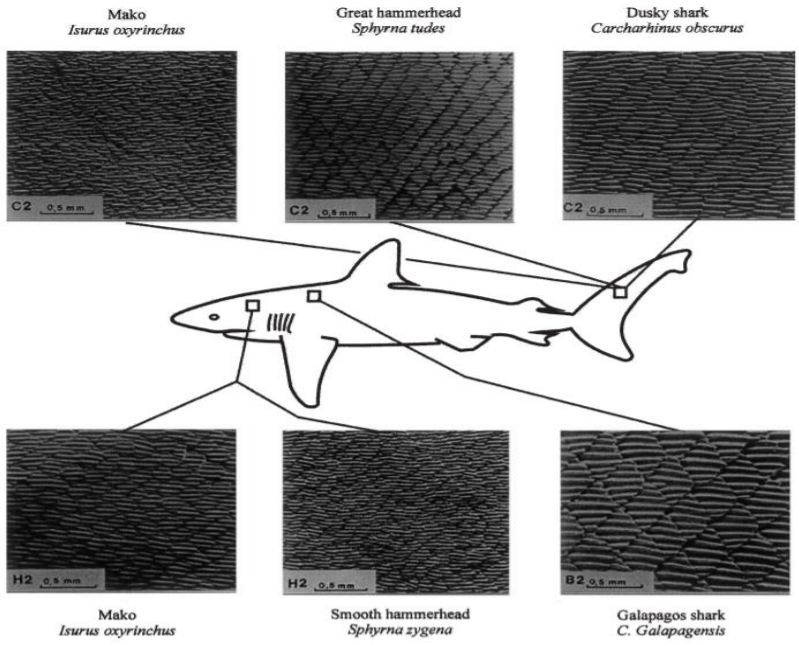

Figure 1 Scale patterns of shark fish [22]

2.2. Surface Texturing Techniques

In this section the previous studies based on ECP, EDM texturing techniques, parameters influencing the texturing and the effect of lubrication on the texturing are discussed.

2.2.1. Electrochemical Processing

In ECP the removal of material takes place through anodic dissolution via electrolysis. The shape of the machining is determined by the shape of the electrode as in case of the EDM [27]. The major benefit in case of the ECP is the smooth surface finish which does not affect any layers, this characteristic of ECP helps in smoothing the micro-metallic products. The low current and a short pulse are required for removing the micro-material, the low currents are produced using the high resistance electrolytes [28].

The electrolytic jet is used as a micro tool and the electrochemical dissolution can be localized by using the high-speed jet. The use of high-speed jet enables the machining of micro indentations with controlled dimensions by switching the current synchronously to the movement of the workpiece. The removal of the material in ECP is atom by atom process. The production cost of the ECP is low, with high efficiency and the absence of the heat affected layer with low tool wear. Hence ECP is more advantageous compared to the other texturing techniques [29]. The schematic representation of the ECP is shown in the Figure 2 along with the sample modifications.

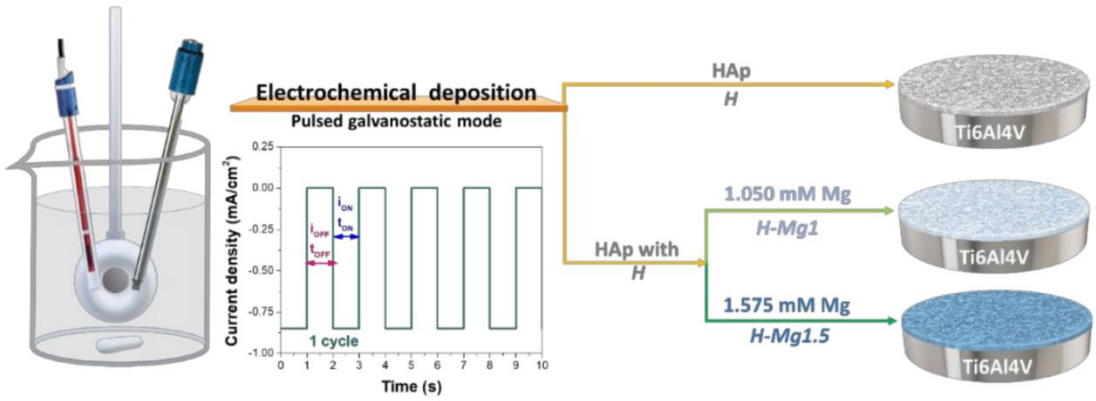

Figure 2 Schematic illustration of the electrochemical deposition process and samples modification [30].

J.C walker et.al., investigated the tribological behaviour of the hyper-eutectic Al-Si cylinder linear material textured with electrochemical jet machining and identified the reduction in COF of 38.5% in the ML regime. In a study by X. Chen et.al., on chrome coated surfaces the friction reduction was achieved on the surface with micro-dimple arrays generated using ECP [31]. Byun et al., used the ECP to fabricate the micro-textures on the bearing steel to

enhance the tribological performance of the steel. The micro dimples of diameter 300μm and depth 5μm was created and found the decrease in the COF [32]. Mishra et al., investigated the surface texturing using ECP in air conditioning and refrigeration compressors under realistic operation condition of starved lubrication where the regular arrays of texture pockets of diameter varying 40-60μm was created. They concluded that the texturing helps in the increase in the scuffing life duration when compared to the non-textured surfaces [33]. Jung won et.al., [34] studied the effect of friction reduction in AISI 440C specimens through micro-ECP texturing method, it was found that the COF was reduced under low-speed conditions for the textured specimens compared to the flat samples. The surface quality and the mechanical properties of the 304 stainless steels were improved by micro-EDM roughing and ECM finishing proving that combining the two processes in milling would increase the machining efficiency [35]. All these studies show the importance of ECM texturing method and its role in improving the surface tribological properties of the materials.

2.2.2. Electric-discharge machining:

EDM is a process of removal of material thermally. The electrical discharge takes between the electrodes of tool and the workpiece resulting in removal of material [28]. The high frequency generated on both the electrodes causes the vaporization of material on the electrodes. The non-conducting dielectric fluid is used as the medium for the material removal process. The functions of the dielectric fluid are to isolate the tool electrode and the workpiece electrode. It helps in enhancing the current density in plasma channel; it also helps in cooling the heated electrodes and removes the discharge particles during the flushing process which helps in preventing short circuit [29].

The main advantages of using the EDM for texturing is that it offers the smaller feature dimension (less than 100μm), complex geometric structures, lower machining, smoother surfaces, greater precision and wider choice of tool material compared to that of the other mechanical processes [30]. The limitations of the EDM is the low material removal rate, the restriction on the size of the workpiece, the achievement of the smaller values of the roughness with longer processing interval, and the incapability of ensuring the dimension of the work piece due to the non contacting nature of the tool and workpiece [31]. In Figure 3 the schematic representation of the EDM is shown.

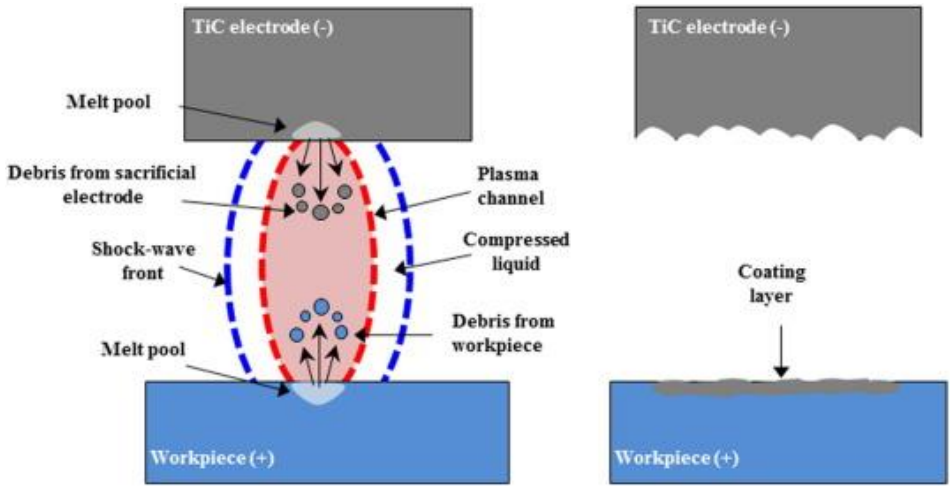

Figure 3 Schematic representation of the EDM mechanism: a) plasma channel formation; and b) workpiece surface modification/coating, following many sparking events [32]

Koshy et al., implemented the surface texturing using EDM to generate the isotropic texture on the tool rake face of the cutting tool. This helps in facilitating the lubricant penetration and retention which reduces the feed and cutting forces thereby enhancing the tribological properties [33]. Kim et al., created the grooves using EDM with depth and width of 50μm and 110μm respectively. The micro pattern decreased the cutting forces which in turn reduced the COF and tool wear. In another study the pattern was created on the tool rake surface using the layer by layer EDM these micro patterns reduced the COF by 9.5-34.5% in comparison to the non-patterned surface and improved the wear by 9.7-11.4% [34]. Zavos et al., used the EDM technique to create the micro texture with a width of 100μm and a depth of 4μm to improve the friction and wear properties in a piston/cylinder assembly. They observed the improvement in the oil film thickness of about 27% [35].

2.3. Surface Texturing Parameters

There are several parameters which contribute in varying the properties in surface texturing, these parameters can be achieved by altering the texture according to the required application. Some of the parameters such as shape, dimensions, direction and spacing between the textures and the testing conditions like speed, lubrication etc. plays an important role in producing the surface textures. Due to the availability of different testing conditions and parameters, there are varying results in different research on the texturing process [44].

The morphology of the texture is an influencing parameter of the tribological properties. Zhan et al., studied the single and the multi-shape textures on dry tribological properties of the 40 Cr steel samples. Six types of textures (dimple, groove, sinusoidal, dimple-groove, dimple-sinusoidal and sinusoidal-groove) were compared for influencing the tribological properties. They found that the tribological properties were affected by different texture morphologies where the dimple-textured surface was found to be having highest COF followed by the groove-textured. Figure 4 represents the different texture shapes used on the substrates for the comparison [45]. Grutzmacher et al., studied the effects of single-scale and multi-scale pattern (multi-scale pattern is implementing two or more different pattern shapes in a material) on the frictional performance of journal bearings. They observed the synergic effect by the multi-scale patterns which improved the frictional performance in comparison with the single-scale pattern [46]. Sasaki et al., studied the effects of the surface texture on the tribological properties of slide ways used for machine tools. They used dimple and groove textures processed using sand blasting technique, they found the COF of the textured surface was smaller compared to the non-textured surface. They explained that the dimple texture played a role of oil reservoir and the parallel grooves prevented the side leakage of the lubricating oil thus contributing in the reduction of friction [47]. Sedlacek et al., studied the influence of geometry and the sequence of the surface texturing process on the tribological properties of the contact surfaces. They investigated the three texture shapes i.e. pyramid, cone, and concave shapes and they found that cone and concave shapes exhibited better tribological properties in comparison with pyramidal shape exhibited. They concluded that sequence of surface texturing has an effect on the tribological behavior that resulted in friction reduction of the samples where the texturing was performed after the coating deposition [48].

Sun et al., studied the influence of micro-textures with different diameters and area density on the tribological properties of the of TC11 alloy at 500^0C. They found that relatively small diameters and dense dimples can likely enhance wear-resistance properties because of the synergistic effect of wear-debris traps and increased oxygen contact area [49]. Xing et al. studied the influence of LST on the frictional pair Si3N4/TiC sliding against steel. They reported that the COF and wear rate decrease by 22.1% and 37%, respectively, with a large texture density of about 70% [50].

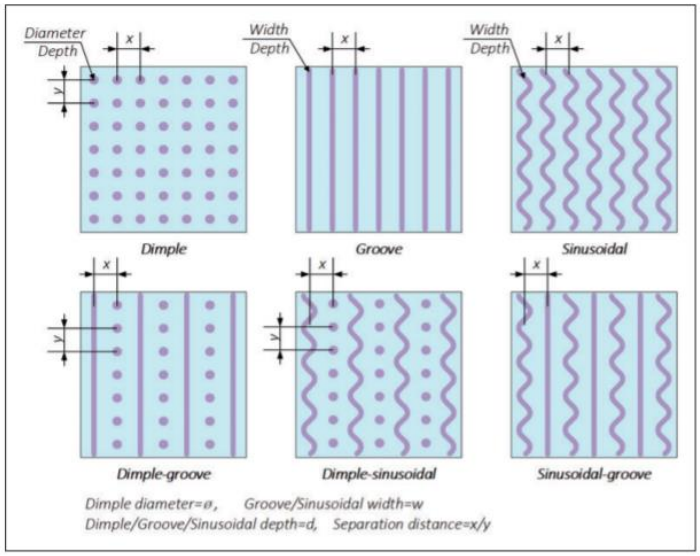

Figure 4 Sketch of different textures on the substrate surface [45].

Apart from texture densities, Rosenkranz et al., also discussed the orientation effects of laser textures on friction in which they concluded that the relative alignment significantly influences friction performance [51]. Rosenkranz et al., further studied the effects of oxide formation, morphology, and nano hardness of laser-patterned steel surfaces influencing the tribological properties [52]. Li et al., studied the effect of laser-textured CuSn6 bronze surfaces with groove, asterisk, and circle textures sliding against polytetrafluoroethylene material under dry friction. Their results show that the friction coefficients of the three different textured surfaces decrease by 10.55%, 6.03%, and 9.5%, respectively [53].

2.4. Surface Texturing Effects on Lubrication

The effect of the surface texture is different in different lubrication regimes. The first study of the surface micro topography on hydrodynamic pressure was found in 1960s for the HL regime, where full film lubrication under low pressure condition is maintained. [54]. The Etsion et al., contributed by introducing the surface texturing in the industrial practice by developing the model to analyze the effect of LST on the friction between the piston and cylinder interface. They showed that the increasing the number of the pockets results in reduced effect of surface texturing on the frictional force [55]. Elastohydrodynamic lubrication (EHL) is also a condition of the full film lubrication under high pressure, there are undesirable effects which occurs due to the surface texturing at EHL contact. The

reduction of pressure is caused by surface texturing at EHL contact which in turn reduces the viscosity of the lubricant reducing the lubricant thickness. Hence the depth of the textures should be lowered than 500nm to attain the good results [56].

In case of the ML condition, the performance of surface textures is difficult to be analyzed. Kovalchenko et al., studied the LST technique to improve performance of friction units under lubrication, they found that the laser texturing expanded the range of speed load parameters under HL which reduced the COF [57]. Amanov et al., studied the tribological characteristics of the dimpled surface processed using ultrasonic nanocrystalline surface modification technique. They found the reduction in COF by 25% and the reduction in wear volume loss by 60% [58]. Rapoport et al., incorporated the solid lubricant in micro dimples on steel surface produced by LST and studied the improvement in the tribological characteristics [59]. D. Braun et al., studied the efficiency of the LST in the friction reduction under ML by producing the dimples on the steel surface and found that the depth-to-diameter ratio showed the nonlinear dependence of COF on the texture diameter, sliding speed and oil temperature [60].

In case of the BL regime, the lubrication occurs due to the asperity to asperity contact between the surfaces hence friction reduction is dependent on the lubricant additives and tribo-film formation. The system is dependent on the wear in order to reduce the friction so altering the surface roughness is crucial therefore both textured size and area has to be reduced [61]. Andersson et al., studied the micro lubrication effect on the steel surfaces processed using the LST. In the BL regime they obtained the best results using high viscosity oil at 8% textured area. However, there was no prominent reduction in the friction due to the trapping of wear debris in the dimples [62].

In case of dry contact conditions, Borghi et al., investigated the tribological effects of surface texturing on the nitriding steel, circular dimples were created using the LST and observed 10% decrease in COF [63]. In a study based on textured wavy pattern on Si_3N_4 / TiC against steel Xing et al., found the reduction in COF up to 22.1% [64]. There are also studies conducted in dry conditions in which Wang et al., studied the effect of micro grooves on the steel surface sliding against the Al2O3 balls in a ball on flat test under dry condition and found the reduction in COF. This reduction was particularly when the spacing between the grooves was reduced and the wear rates were reduced compared to the non-textured surfaces

[65]. Kang et al., studied the nano and micro dimple textures on the aluminium surface under dry condition and found the increase in COF by twice the non-textured surface [66]. Hence there is no clear rule on improving the COF; however, parameters like texture space, size and depth are worth studying.

2.5. Surface Coating

Surface coating has been proved as one of the surface modification techniques that as evolved over time. There are various types of coatings depending on the applications, based on this the coatings can be varied using various deposition techniques that includes the PVD, chemical vapour deposition, ion implanting, electrolytic deposition etc. Coatings can also be categorized based on the coating parameters such as the material deposited, components in deposition, phases and layers. The main goal of this evolving nature of the coating research is to improve the various mechanical and tribological properties of the materials. Surface coatings also help in acting as the solid lubricant in the material interface between two samples in contact that helps in friction reduction and improving the tribological properties. One such coating that has recently identified is the TMD coatings, which will be studied in this section in detail.

2.6. PVD - Magnetron Sputtering

PVD is one of the surface coating technique that has been known for over 100 years [67]. It is a process of film deposition where the coating is grown on the substrate atom by atom. In this technique vaporization of the destined coating material occurs which gets deposited on the surface of the target material. This process helps in changing the surface properties and creates the transition zone between the substrate and the coated material. The substrate material affects the properties of the film, the deposition of the material can be made under different atmospheric conditions such as vacuum, plasma, gaseous etc [68]. PVD is one of the excellent vacuum coating process which helps in improvement of corrosion and wear resistance [69]. It is applicable in various mechanical tools, optical enhancement, moulds and dies etc. This process can deposit different layers of coating such as mono-layered, multi-layered and also multi-graduated coatings with special alloy compositions. Their

flexibility in adapting this technique to the market demands has further improved this technique [70]. In PVD technique, a thermal physical process is used in releasing or collision of the material to be deposited on the target substrate. The gaseous plasma in a vacuum environment is one of the medium in which the deposition of coating takes place which helps in better composition control of the deposited film [71]. Figure 5 represents the schematic drawings of the PVD process.

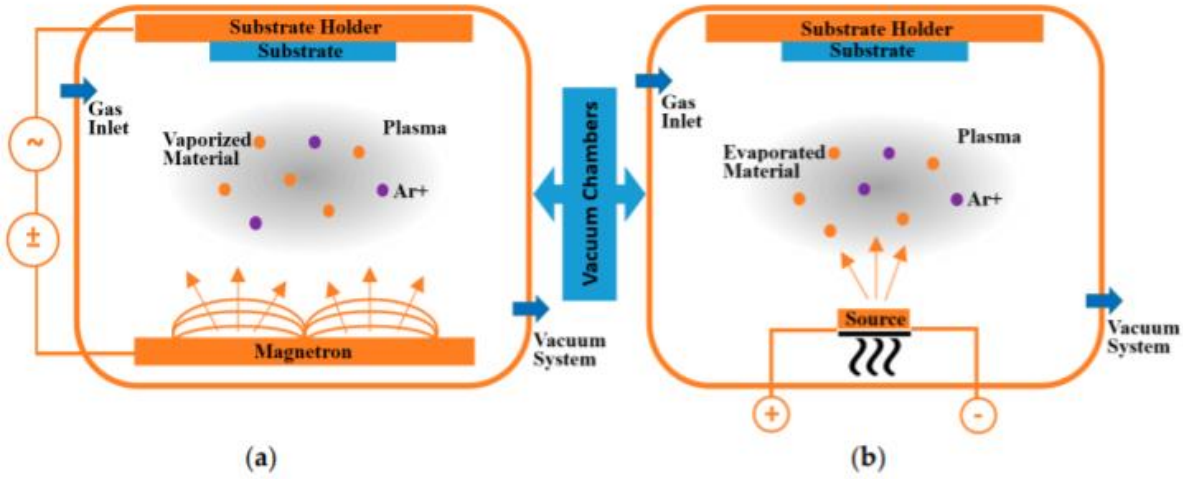

Figure 5 Schematic drawing of two conventional PVD processes: (a) sputtering and (b) evaporating using ionized Argon (Ar+) gas [72].

PVD is the basic principle of the sputtering technique in which the coating is performed by substrate material on the target by bombardment of the high energetic ions generated using glow discharge plasma [73]. Magnetron sputtering is a high-rate vacuum coating technique for depositing metals, alloys, and compounds onto a wide range of materials with thicknesses up to millimetres. It exhibits several important advantages over other vacuum coating techniques, a property that led to the development of a large number of commercial applications from microelectronic fabrication to simple decorative coatings. In this technique the deposition takes place by condensation of the substrate material which gets deposited on the target with the help of magnetic field which is parallel configured to the target that constrains the motion of the secondary electron to the vicinity of the target surface. This technique solves the limitations of the traditional sputtering technique where there was no medium to direct the material deposition on the surface and hence increases the ionization efficiency by increasing the higher bombardment rate of ions on the target [74].

2.7. TMD Coatings

The most widely used coating for the application of solid lubrication is the TMD coating; the transition metals used in these coatings shows better anti frictional properties under dry-friction conditions. The main reason for this is the presence of the hexagonal crystal structure. The metals such as molybdenum (Mo), tungsten (W) and niobium (Ni) with disulphides and diselenides belongs to TMD family [75-76]. In order to use the TMD as a friction reducing agent it has to be either used as an oil additive or a coating. There are various researchers who have studied the TMD coatings in order to improve frictional properties. Polcar et.al. [77] have studied the TMD-C nanocomposite coatings that provided the strong evidence of friction reduction in sliding at ambient condition that was evaluated by analyzing the formation of low-friction tribolayer at the cross-section of the sliding interface of the coating. Most of the literatures have concluded that the sole reason for the formation of the low friction tribolayer is due to the reorientation or the crystallization of the TMD's inside the coating, or near to the contact interface as a thin layer on the top of the surface [78-81]

2.7.1. MoSeC Coatings

MoSeC is a type of TMD-C coatings which is known for its rich combination of optical, electrical, mechanical and tribological properties [82]. $MoSe_2$ is ductile in nature and sustains high deformation before fracture also it is elastically anisotropic [83]. Furthermore, due to its poor oxidation resistance which is the result of lower activation energy it only gets activated at higher temperatures. With the mentioned mechanical advantages of the MoSeC it is suggested that the substrate doping is needed to achieve the favorable tribological properties at a temperature of up to 300^{o}C in all the environment conditions (i.e., vacuum, dry and humid environments) [84]. Jorge Caessa et.al., investigated the micro structural, mechanical, and tribological properties of the MoSeC coating against rubber and found that the MoSeC improved the frictional property [85].

2.7.2. WSC Coatings

WSC coating is a type of TMD-C coatings that is deposited on the mechanical components to provide the solid lubrication on the surfaces. Tungsten disulphide (WS_2) belongs to the

class of transition metals with the poor shear strength due to large anisotropic crystal structure consisting of hexagonal crystal structure with tungsten atoms sandwiched between the two layers of sulfur atoms [86-87]. However, it is found that the mechano-tribological properties of this coatings can be increased by alloying it with various metals such as titanium (Ti) and chromium (Cr) and non-metals such as carbon (C) and nitrogen (N). [88-90]. Tomas polcar et.al., studied the friction and self-lubricating properties of the WSC coating in a sliding condition by increasing the load and found that friction mechanisms of the WSC coating is fundamentally different from pure TMD coatings. Sulphur/tungsten (S/W) ratio in WSC coating plays an important role in affecting the tribological performance of the sample, higher the S/W ratio then better the tribological property [91].

2.8. Synergy of Surface Texturing and Coating:

Amanov et al., studied the tribological characteristics of the Si-DLC coating using LST under oil lubricated point contacts and found that the textured Si-DLC coating decreased the friction and wear when compared to non-textured Si-DLC coated sample. The test was conducted under certain temperature range which has attributed the effects of dimples and microstructures due to high energy action of the pulsating laser beam [92]. Meng et al., studied the tribological performance of the cemented carbides by combining LST along with WSC solid lubricant coating and found that the texture captures wear debris in the grooves during sliding condition. In addition to which the lubricant coating between the grooves contributes sufficient lubricant within the contact zone improving the friction and wear performance of the cemented carbides [93]. Ze Wu et al., studied the properties of the dimple-textured titanium alloys under dry lubrication condition. They concluded that the textured surface filled with the solid lubricant reduced the wear loss in titanium samples and adhesion on the steel counterpart also they found that the distance between the dimple texture plays an important role on anti-friction and anti-wear properties [94].

Okasanen et al., studied the enhancement of tribological properties of the tetrahedral amorphous carbon TaC films at elevated temperature by LST and burnished with WS_2 addition on steel samples. They found that the texturing improved the wear life of the TaC and WS_2 surfaces by more than two times compared to non-textured surfaces [95]. In a study on surface texturing for adaptive solid lubrication on steel samples, Basnyat et al., found

implementing micro dimple patterns of different sizes on the TiAlCN hard coatings produced by cathodic arc vacuum evaporation technique resulted a significant change in the tribological properties. The properties such as friction and wear were found to significantly decrease at 25^0C and 570^0C temperatures. This temperature adaptive behavior was found by the solid lubrication which was entrapped in the simple textures [96].

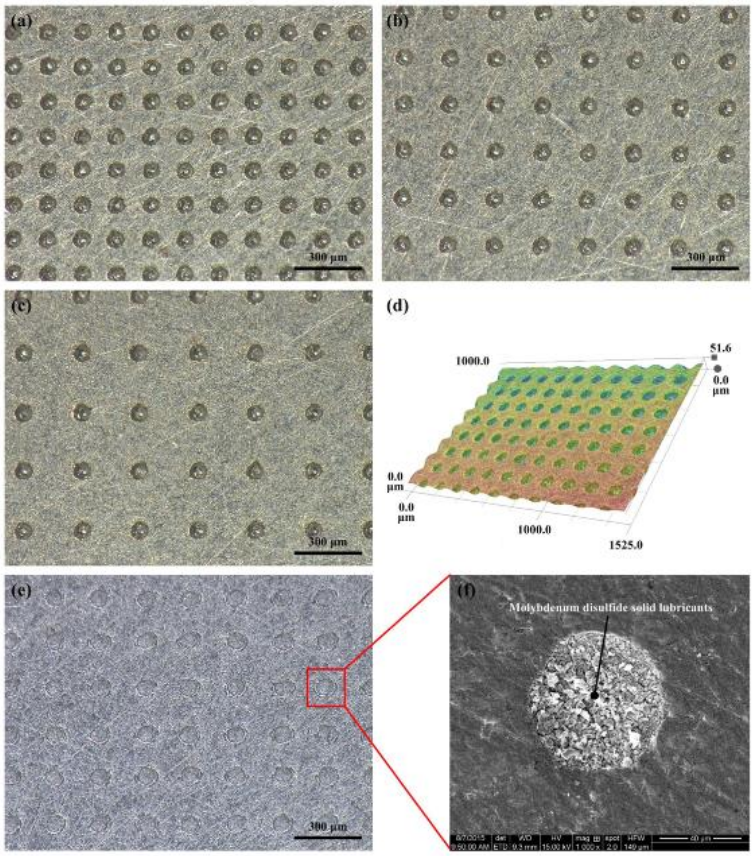

Figure 6 The dimple patterns with different dimple-distance: (a) T-D150, (b) T-D200, (c) T-D250, (d) stereoscopic profile of TD-150, (e) T-D200 sample filled with molybdenum disulfide and (f) enlarged view of single dimple filled with solid lubricants [97].

These studies have shown that combining the texturing along with the surface coating increases the tribological characteristics of the materials.

2.9. Research Gap

The literature reviews as reviled the importance of the ECP and EDM texturing techniques and TMD coatings on improving the frictional properties on the materials surface. However,

it is also noted that these techniques individually have improved the tribological properties in selected lubrication regimes

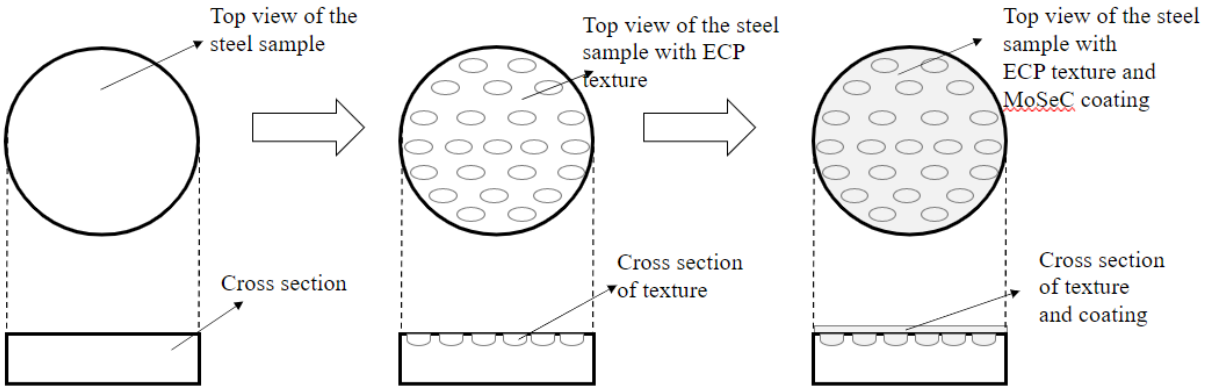

Figure 7 The schematic representation of the sequence of the techniques used in this study.

So, it is important to investigate the effect of these techniques when combined and understand their influence and verify their strengths in all the lubrication regimes. The different geometric parameters that affect the role of texturing are also conducted in this study to compare the best pattern that fetches the better tribological behavior. Figure 7 shows the schematic representation of the step by step procedures followed in this investigation.

CHAPTER 3

3. EXPERIMENTATION

In this chapter, the details on preparing the electrodes, samples, chemical composition of samples along with their physical parameters are explained. After the electrode and sample preparation the sample has to be textured hence the information on the texturing technique, type of electrodes used, the dimensions of the geometric patterns and the procedure for the texturing are listed. Further the coating techniques, the chemical composition of the coatings along with the various physical parameters involved in the coatings are mentioned. The block-on-ring tribometer test that is used to analyze the tribological properties of the samples are explained and the calculation involved in plotting the Stribeck curves and different lubrication regimes are discussed.

3.1. Electrode and Sample Preparation

Electrodes are prepared using the graphite material and were textured using a fibre laser (Nd:YAG) which has a maximum power of 6W at 20kHz, a spot size of 3μm, a pulse width of 35ns, and a repetition rate of 20kHz. The wobble diameter and amplitude were kept constant and designs for conical cylinders were used that were produced by corel draw design software. The variables in this process were power, scanning speed, and number of passages. Initially optimization took place for both designs followed by processing of the graphite electrode textures. Furthermore, these textures would be used for replication on the steel sample by ECP and EDM+ECP techniques.

Table 1 Chemical composition of steel specimen

Elements	C	Cr	Mn	Mo	V	Si	W
AISI M2	1.00	4.15	0.30	5.00	1.95	0.30	6.25

The sample material used in this investigation is the AISI M2 steel; it is molybdenum based high speed steel that belongs to tungsten-molybdenum series. The average chemical composition of this is mentioned in the Table-1.

The samples of 24 mm diameter and 7.9 mm thickness are obtained and it is quenched followed by tempering before the texturing on its surface. Further, the samples are polished to a mirror finish with a roughness of 0.04 μm and are cleaned in acetone and ethanol medium for 15 mins each. The prepared samples are textured; once the samples are textured it is further cleaned with the acetone and ethanol medium for 15mins each before coating.

3.2. Texturing with ECP and EDM + ECP

The samples prepared are textured with ECP using three different electrodes to obtain the three geometric patterns. Before texturing the samples are cleaned with ultrasonic bath for 15mins in ethanol and acetone medium and were textured with required texture geometry as per the electrode pattern. The shape of each electrode was replicated on each sample forming the ECP samples. The electrodes possessed the identical geometric pattern that has to be textured on the samples. Electrodes with three different texture patterns were used where, two electrodes have rectangular patterns with different dimensions i.e., electrode-1 (E1) and electrode-2 (E2) and one electrode with circular pattern i.e., electrode-3 (E3). The dimensions of the electrodes were characterized using SEM, the electrode E1 with rectangular pattern had the dimension of length- 167μm, breadth- 158μm, E2 with rectangular pattern had length-158μm, breadth-156μm and E3 with circular pattern had diameter-138μm. One sample was produced from each electrode using ECP process namely ECP_S1, ECP_S2 and ECP_S3 from E1, E2 and E3 respectively.

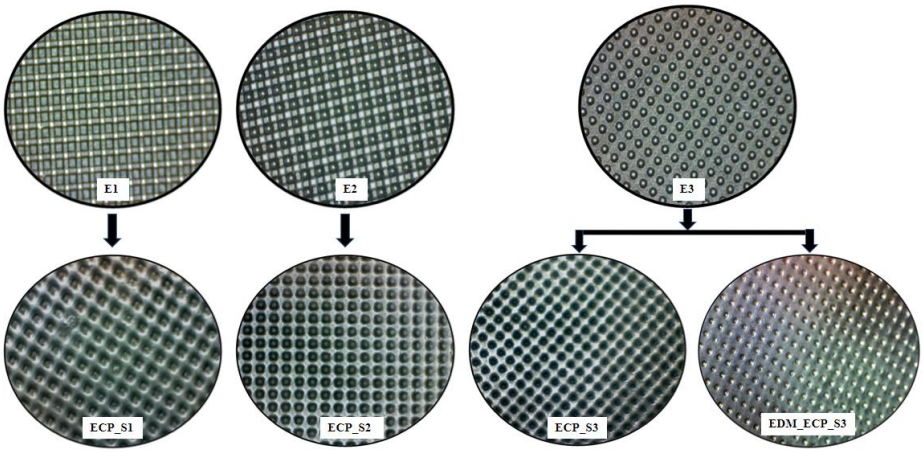

Figure 8 Surface images of the electrodes and specimens

In case of the EDM+ECP texturing technique similar cleaning process was performed for the sample followed by the texturing. However, the texturing was performed in a sequence,

where the samples were textured with ECP followed by EDM technique. The reason for this sequence was to avoid the erosion wear on the samples. In this technique sample EDM_ECP_S3 was produced with E3 electrode.

All the obtained samples were tested for their tribological properties using block-on-ring tribometer and then they were coated with MoSeC coating to test the effect of coating on the textures of the ECP samples and EDM+ECP sample was coated with both MoSeC and WSC films to check their behaviours. Figure 8 shows the images of the textures and samples created after texturing process.

3.3. Coating with MoSeC and WSC Films

The textured samples were coated with the two TMD films i.e., MoSeC and WSC films, for the samples obtained from the ECP texturing the coating was performed using the MoSeC film and the sample obtained with the dual texturing technique EDM+ECP was coated with both MoSeC and WSC films. The deposition of the MoSeC and WSC coatings were done with a closed-field unbalanced magnetron sputtering in a semi industrial unit (Teer Coatings Ltd. UDP650/4, UK) at institute of pedro nunes (IPN). The volume of coating deposited was about 275dm^3 with four targets (340 x 140 x 8mm) mounted on the magnetrons which were arranged vertically on the chamber walls. In case of MoSeC coating two graphite targets were used with one $MoSe_2$ target and one Chromium (Cr) target (the chromium target was used for the deposition of the interlayer) Similarly, for WSC coating two graphite targets were used with one WS_2 and one Cr target. In both coatings the cleaning of the targets and the substrates were done in argon (Ar) gas atmospheric medium at a pressure of 0.5Pa then the deposition of the elements was performed. The targets and substrates were powered by DC power supplies (Advanced energy pinnacle, USA) at IPN, they operated in power control mode. The distance between the target and the substrate was around 25cm and the bias voltages were maintained to 0V with deposition time of 120mins and deposition rate of 13.8nm/min. For MoSeC coating, the deposition was made with10min Cr interlayer, 10 min gradient layer and 100 min MoSeC and obtained the thickness of 1.8μm on all the three ECP textured samples and one EDM+ECP dual textured sample. However, in WSC coating, deposition was made with 10 min Cr interlayer, 10 min gradient layer and 100 min WSC and obtained the thickness of 1.3μm on the EDM+ECP dual textured sample. The average

chemical composition of the coatings along with the coating parameters are summarized in the Table 2.

Table 2 Chemical composition and properties of the coating

Coating	V_B	Elemental Composition (atomic %)							Thickness (µm)	D_t (m)	D_r (nm/m)	Hardness (GPa)
		C	Se	O	Mo	W	S	Cr				
MoSeC	0	58.0	26.9	0.9	12.5	--	--	0.2	1.8	120	13.8	4.3
WSC	0	58.5	--	2.8	--	14.4	22.3	0.3	1.3	120	10.8	4.8

The textured coated samples are named as ECP_S1', ECP_S2' and ECP_S3' in case of ECP-MoSeC coating and EDM_ECP_MoSeC_S3' in case of EDM+ECP-MoSeC coating. For WSC coating on dual textured sample (EDM+ECP-WSC) it was named as EDM_ECP_WSC_S3'. Further these samples were tested for their tribological behaviors and their performances were compared with the only-textured samples. Figure 9 shows the schematic representation of the top view of the magnetron sputtering chamber used in the similar kind of TMD film deposition.

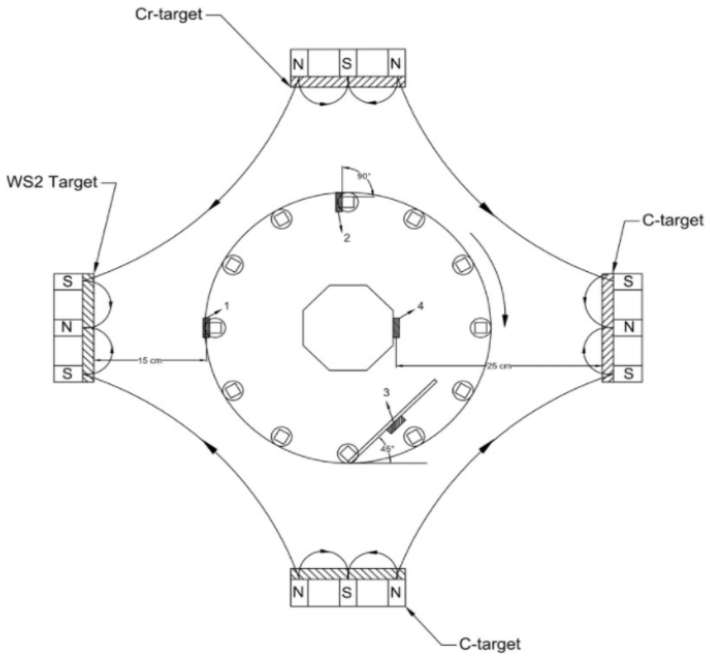

Figure 9 Top view of the sputtering chamber during the deposition process [91]

3.4. Block-on-ring Experiments

The tribological characteristics of the specimens were tested using the block-on-ring test. Block-on-ring tribometer is a widely used technique to evaluate the sliding wear behaviors of the materials in different conditions which allows the reliable ranking of the material for specific tribological applications. Sliding wear involves in a complex wear mechanism on the contacting surface which causes adhesion wear, two and three body abrasion wear and fatigue wear mechanisms. These wear behaviors are influenced by the various parameters such as working environment including normal loads, speed, corrosion and lubrication. Using the block-on ring-tribometer one can evaluate the wear on the contacting surface. Figure 10 shows the schematic representation of the block-on-ring setup. The setup consists of a rotating ring, sample holder, lubricant reservoir, load cells to measure the voltage change and the speed controlling system for the rotating disc.

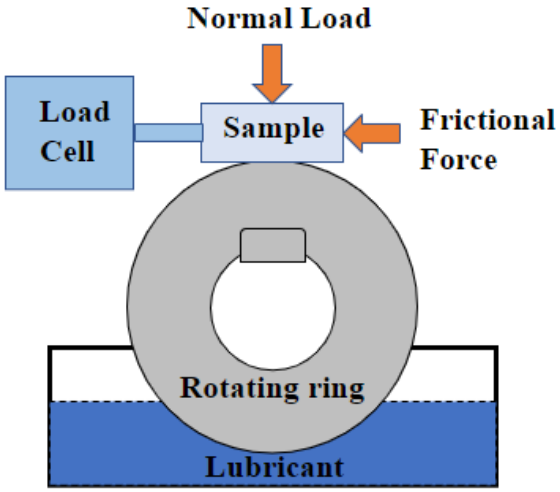

Figure 10 Schematic representation of the block-on-ring setup

The test was performed on a constant load condition by applying 25N stationary load on the sample against the rotating ring made of AISI 3145 steel with the initial surface roughness of 0.04μm and diameter of the ring is 150mm and thickness is 12mm. The average chemical composition of the ring is given in the Table 3.

Table 3 Chemical composition of the counter body (ring)

Elements	C	Cr	Mn	Ni	Si
AISI 3415	0.17	0.75	0.55	3.25	<0.20

The test was performed by placing the sample and the ring in contact and the interface is loaded with 25N stationary load and in a lubricated condition with the lubricating oil of the viscosity 0.099Pa-s. The rotation of the ring is varied with different speeds which are in the range of 0.01-0.47m/s, and the COFs for each speed is noted to understand the friction behavior in all the lubrication regimes. The lubrication regimes of the samples are understood by plotting the Stribeck curves (the Stribeck curve is the plot between COF v/s Hersey number). And hence the performances of the coated and uncoated samples are compared for the changes in its frictional properties in all the lubricated regimes. Further, the lubrication regimes can also be understood by calculating the Tallian parameters at each speed which will give us further explanation on the distribution of the lubricated regimes and their COF values. Figure 11 shows the schematic representation of the block-on-ring setup used in this experiment.

Figure 11 Schematic representation of the block-on-ring setup used.

The Hersey number is calculated using the dynamic viscosity of the oil, applied load and the entrainment speed of the oil using the equation-1

$H = \frac{\eta * N}{P}$ 1

where,

η is dynamic viscosity of the oil [Pas]

N is entrainment speed of the fluid [m/s]

P is the normal load per unit length of the tribological contact [N/m]

In Hersey number to calculate η equation-2 has been used

$$\eta = \nu \times \rho \quad \text{..... 2}$$

where,

ν is kinematic viscosity of the oil [m^2/s]

ρ is density of the oil [kg/m^3]

In Hersey number to calculate N equation-3 has been used

$$N = 2 \times \pi \times \frac{RPM}{60} \times r \quad \text{..... 3}$$

where,

r is radius of the ring [m]

In Hersey number to calculate P equation-4 has been used

$$P = \frac{N}{t} \quad \text{..... 4}$$

Where,

N is normal load [N]

T is the thickness of the ring [m]

The understanding the lubrication regimes using the Stribeck curves are limited to the number of parameters considered in the Hersey number calculation and hence the better understanding would be using the Tallian parameter which considers the various parameters of the surface contact interface. The Tallian parameters can be calculated by using the ratio of minimum film thickness and the surface roughness values using the equation-5

$$\lambda = h_0(\sigma a^2 + \sigma b^2)^{0.5} \quad \text{..... 5}$$

Where,

λ is the Tallian parameter,

h_0 is the minimum film thickness [m]

σ_a rms value of block roughness [m]

σ_b rms value of ring roughness [m]

The minimum film thickness h_0 is given by the Hamrock Dowson equation assuming the direction of the counter surface of the ring on the sample is along the entraining velocity of

the ring in the oil and parallel to the minor contact axis of the elliptical contact at the interface which is given by the equation-6.

$$\left(\frac{h}{R}\right) = 3.63 \left(\frac{U\eta 0}{E'R'}\right)^{0.68} (\alpha E')^{0.49} \left(\frac{W}{E'R'^2}\right)^{-0.073} \left(1 - e^{-0.68k}\right) \quad \ldots\ldots\ldots\ldots\ldots 6$$

Where,

U is entraining surface velocity [m/s]

E' is reduced young's modulus [Pa]

R' is radius of curvature [m]

α is pressure-viscosity coefficient [m^2/N]

W is contact load [N]

k is ellipticity parameter.

CHAPTER 4

4. RESULTS AND DISCUSSIONS

In this chapter, the characterizations of the electrodes and the specimens before the tribological testing are performed with optical profilometer to determine dimensions of the textures on the electrode and the specimen. Tribological test, block-on-ring results on different smooth, coated, textured and textured/coated specimens with non-additive lubricant oil have been presented. A detailed discussion has been made on the obtained modification in COF in different regimes. To analyze the effect of this test on the surface of the specimen, the tested specimens were analyzed using SEM micrograph with EDS.

4.1. Geometry of the Electrodes and Specimens

Since the electrode geometry is going to replicate on the specimen surface therefore, it is very important to analyze the dimensions of the prepared electrodes. Similarly, as mentioned earlier that the textures pattern, size, shape make significant difference in the tribological behavior of the material. Here, the electrodes and the specimens were performed using two different techniques, SEM (the high-resolution merlin scanning electron microscope by ZIESS) and 3D optical profilometer (Alicona infinite focus 3D microscope). With the help of surface profile obtained via 3D profilometer the parameters such as the texture length (D_l) breadth (D_b), diameter (D), depth (D_d), height (D_h) and the spacing between the two adjacent textures (D_s) have been optimized. The surface morphology of electrodes and the textured specimens have been analyzed with SEM.

4.1.1. Electrode Characterization

The surface morphology of the three electrodes Electrode 1, Electrode 2 and Electrode 3, respectively has been analyzed with SEM showed in Figure 12. From these micrographs it is clear that the geometry of these electrodes is rectangular for electrode 1 and 2, whereas

circular for electrode 3. To optimize the texture parameters surface profile is taken as showed in Figure 13.

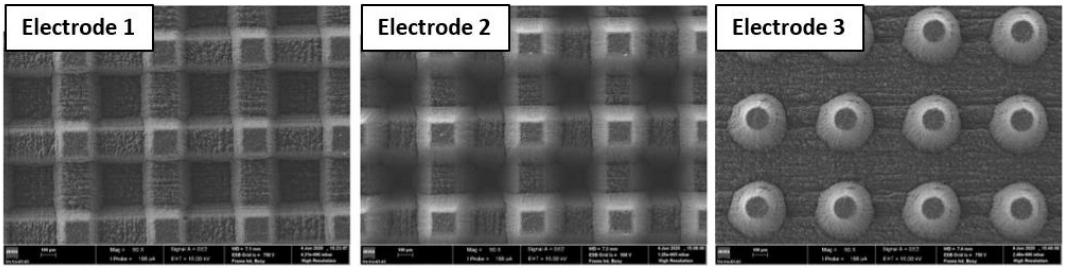

Figure 12 The SEM surface images of the electrodes 1, 2 and 3, respectively

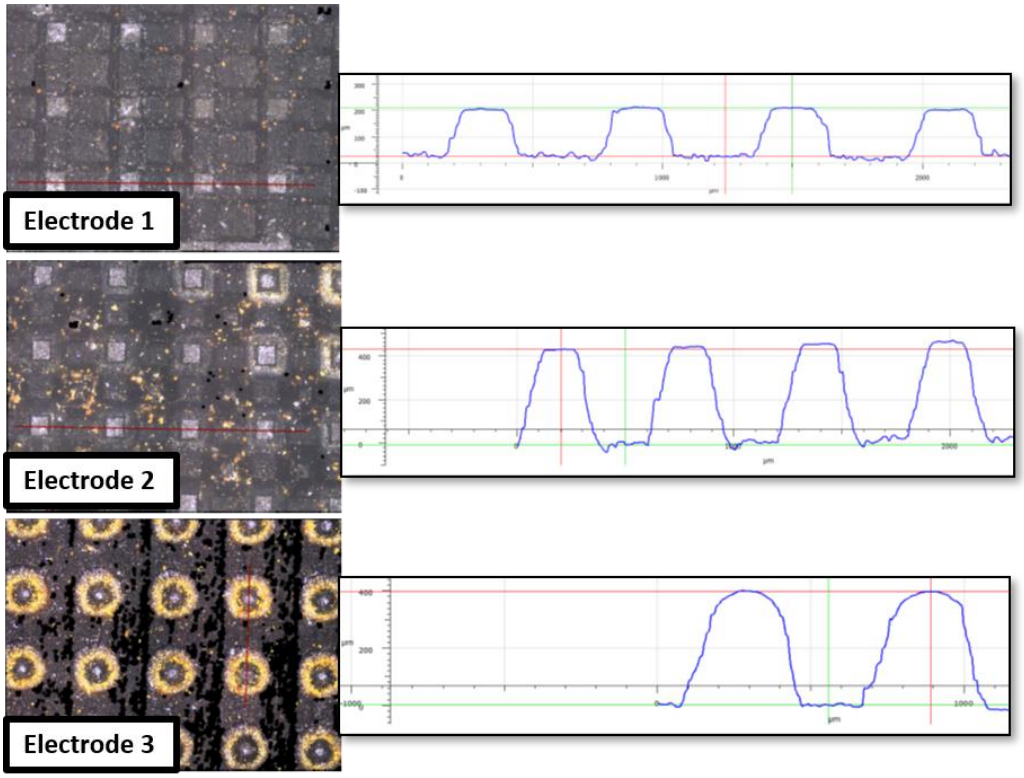

Figure 13 Surface profile images of the electrodes

After analyzing these surface profiles, the calculated average values of dimensions of the textures on the electrodes 1, 2 and 3 are tabulated in Table 4.

Table 4 Geometry of textures on the electrodes.

Electrodes	D_l (µm)	D_b(µm)	D (µm)	D_h(µm)	D_s(µm)
Electrode 1	167	158	-	193	589
Electrode 2	156	158	-	383	571
Electrode 3	-	-	138	402	591

4.1.2. Sample Characterization

The surface morphology of the three electrodes Electrode 1, Electrode 2 and Electrode 3, and their replication on the specimen named ECP_S1, ECP_S2 ECP_S3 and EDM_ECP_S3 has been already shown in Figure 14. Here in figure 14, the surface and profiles for ECP_S1, ECP_S2 ECP_S3 and EDM_ECP_S3 has been shown. The specimen's surfaces were highly reflective to obtain the proper image due to the polishing that was performed after the texturing to remove the surface asperities.

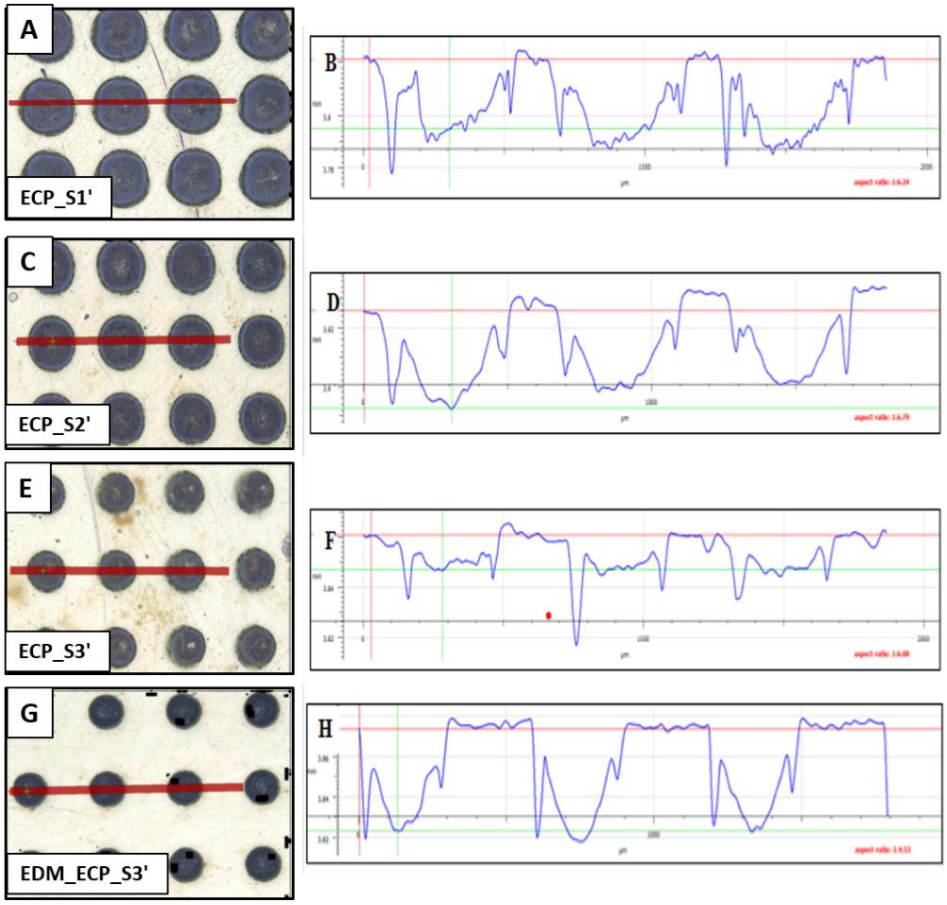

Figure 14 The Surface profiles of all the textured specimens; A&B(ECP_S1), C&D (ECP_S2), E&F (ECP_S3) and G&H (EDM_ECP_S3)

The sample ECP_S1 is replicated by E1 with the rectangular dimple pattern as shown in the Figure 14A, the surface texture profile for ECP_S1 is shown in the Figure 14B. The dimple dimensions of ECP_S1 are D_l - 402µm, D_b -424µm, D_d – 21µm and D_s – 154µm. The specimen ECP_S2 textured with the E2 with the rectangular dimples shown in the Figure 14C, and its texture profile is shown in the Figure 14D. The dimple dimensions of the ECP_S2 are D_l - 356µm, D_b -384µm, D_d – 31µm and D_s – 188µm. Similarly, the sample

ECP_S3 textured by the E3 and is shown in the Figure 14E, and its texture profile is shown in the Figure 14F. The dimple dimensions of ECP_S3 are D - 262µm, D_d - 19µm and D_s - 306 µm. EDM_ECP_S3, dual textured circular geometry with EDM and ECP is shown in the Figure 14G with surface profile in Figure 14H, respectively. The dimensions of the EDM_ECP_S3 are D-268µm, D_d - 59µm and Ds -331µm. Average values of the dimensions of all the specimens are summarized in the Table 5.

Table 5 Geometry of textures on the specimen**.**

Specimens	D_l(µm)	D_b(µm)	D(µm)	D_d (µm)	D_s(µm)
ECP_S1	402	424	-	21	154
ECP_S2	356	384	-	31	188
ECP_S3	-	-	262	19	306
EDM_ECP_S3	-	-	268	59	331

4.2. Block-on-ring

All samples were submitted to the tribological testing, block-on-ring experiment with lubricant oil without additives of density around 0.099 Pa-s at room temperature at sliding speeds 1.5 RPM, 2.5 RPM, 3.5, RPM, 5 RPM, 10 RPM, 20 RPM, 30 RPM, 40, RPM and 60 RPM as described in chapter 3. The Hersey number (HN) were calculated for each rotating speed to plot the Stribeck curve between Hersey number and observed COF for all the smooth, coated, textured and textured/coated specimens. The performance of the specimens is determined by analyzing the Stribeck curve and the lubrication regimes present on the curve. The lubrication regimes such as BL, ML and HL regimes can also be studied using the Tallian parameter (λ) values. For calculating λ, minimum thickness of the film (h_0) between the interface plays very important role therefore, h_0 and λ have been calculated for each sliding speed that help in determining the lubrication regimes tabulated in Table 6. The BL regime is obtained at the lower speeds in the range of 0.01- 0.02m/s with the very least minimum film thickness values ranging 3.12×10^{-08}to5×10^{-08}m with Tallian parameter values of 0.7-1.1 at this regime the interface of the sample and the ring is in contact with improper lubrication resulting in higher COF values compared to the other regimes. In case of ML regime; it falls in the nominal speed range which is around 0.03-0.16 m/s. In this regime there is formation of film thickness that is very partial and it is in the range of 6.59×10^{-08} to 2.06×10^{-07} m and the Tallian parameter values ranges within 1.4-2.5. However, in case of the HL regime the COF values are comparatively low in comparison to other regimes

because of the formation of the lubricating film with the thickness range of $2.63\times10^{-07}$to 4.28×10^{-07}m. This regime is formed when the interface is at high speed (0.23-0.47 m/s) and the Tallian parameter value for these regimes comes out to be from 5.7-9.2. These lubrication regimes are very important to analyze the frictional properties of the specimens.

The reduction in the COF values results in better frictional properties of the specimens and hence the Stribeck curve with lower elevation is considered as the better performing sample. Further, the comparisons of these curves are performed for various specimens based on the texture geometry, coating / without coating with the smooth and only coated specimens. The percentage improvement for all the specimens is calculated keeping the smooth sample has the reference. These comparative graphs along with the percentage improvement in the specimens are discussed in this section. The calculated value of Hersey numbers, minimum film thickness along with the Tallian parameter for the different speed range is tabulated in the Table 6.

Table 6 Calculated values of HN, h_0, λ and lubrication regimes**.**

RPM	**1.5**	**2.5**	**3.5**	**5**	**10**	**20**	**30**	**40**	**60**
Speed(m/s)	0.01	0.02	0.03	0.04	0.07	0.16	0.23	0.31	0.47
HN	2.24E-05	1.49E-05	1.12E-05	7.46E-06	3.73E-06	1.87E-06	1.31E-06	9.33E-07	5.60E-07
h_0(m)	3.12E-08	5.00E-08	6.59E-08	8.02E-08	1.17E-07	2.06E-07	2.63E-07	3.23E-07	4.28E-07
(λ)	0.7	1.1	1.4	1.7	2.5	4.4	5.7	7.0	9.2
Lubrication Regimes	**Boundary lubrication**		**Mixed lubrication**			**Hydrodynamic lubrication**			

4.2.1. COF Variation for Smooth/Coated Specimens

Surface coatings are used to modify the surface properties of the surface that affects their tribological behaviors. The TMD coatings used in this study are the MoSeC and WSC which are coated on the smooth specimen named as MoSeC_S0' and WSC_S0' respectively, to analyze the influence of coating as compared to smooth specimen. These smooth (S0) and coated MoSeC_S0' and WSC_S0' are tested on block-on-ring test for their frictional behaviours to verify the efficiency of these coatings. Figure 15 shows the Stribeck curves of S0, MoSeC_S0' and WSC_S0' specimens and improvement in COF can be seen in both coated MoSeC_S0' and WSC_S0'specimens in BL regime as the surfaces at the interface will be in contact to each other with lower lubricated film thickness. The improvement is found to be in the range of 12-13 % and 15-35 % for MoSeC_S0' and WSC_S0' respectively

in comparison to S0. The performance (%) of S0, MoSeC_S0' and WSC_S0' is tabulated in the Table 7.

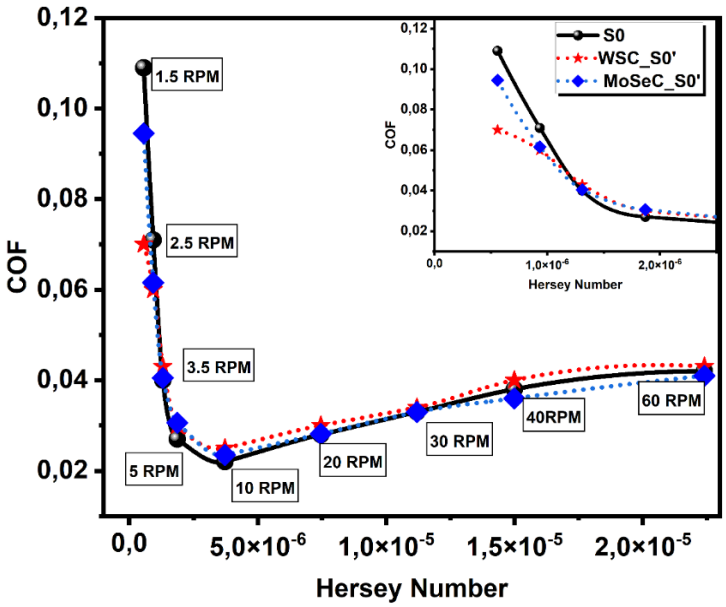

Figure 15 Stribeck curves of the S0,MoSeC_S0' and WSC_S0'

This objective of improving the frictional properties at the BL regime by coating is successfully achieved with these coatings. In case of ML regime, it is found that COF values are very much similar to the S0. However, in case of HL regime for MoSeC_S0' the frictional properties have been elevated to 4.7 % and 1.9 % for sliding speeds 40 and 60 RPM, respectively. These improvements of COF values in case of BL and HL regime for MoSeC coating is very interesting to use on textured specimens for optimizing the synergy of texture and coating on tribological behavior in different regimes.

Table 7 Performance of the MoSeC_S0', WSC_S0' sample in comparison to S0

RPM	1.5	2.5	3.5	5	10	20	30	40	60
MoSeC_S0'	**13.3 %**	**12.7%**	-1.2%	-13.3%	-6.8%	-0.5%	-0.3%	**4.7%**	**1.9%**
WSC_S0'	**35.8%**	**15.5%**	-7.5%	-11.1%	-13.6%	-7.1%	-3.0%	-5.3%	-2.4%
S0	--	--	--	--	--	--	--	--	--

4.2.1. COF Variation for Textured Specimens

The texture geometry plays an important role in influencing the tribological properties. Hence, it is important to analyze all these three ECP textured geometries with Block-on-ring test to find out which texture geometry is making significant improvement.

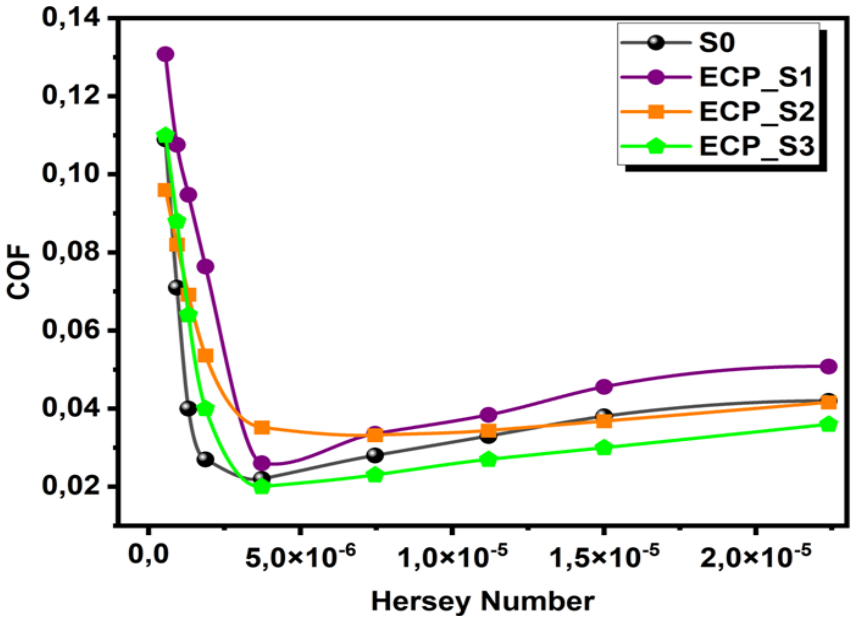

Figure 16 Stribeck curves of the specimens S0, ECP_S1, ECP_S2 and ECP_S3

Figure 16, shows the Stribeck curves of smooth S0 and ECP textured ECP_S1, ECP_S2, ECP_S3 specimens. From the Stribeck curve it is observed that circular textured specimen ECP_S3 is exhibiting lower COF in HL regime as compared to S0. The percentage improvements compared to S0is tabulated in the Table 8.

Table 8 Performance of the ECP samples in comparison to S0

Specimen	RPM	1.5	2.5	3.5	5	10	20	30	40	60
ECP Textured	ECP_S3	-0.9%	-23.9%	-60.0%	-48.1%	**9.1%**	**17.9%**	**18.2%**	**21.1%**	**14.3%**
	ECP_S2	-17.4%	-50.4%	-124.0%	-142.9%	-25.4%	-4.3%	**1.8%**	**4.2%**	**2.8%**
	ECP_S1	-20.0%	-51.5%	-137.0%	-182.9%	-18.2%	-20.0%	-16.4%	-20.0%	-20.9%
Smooth	S0	-	-	-	-	-	-	-	-	-

The improvement is about 14-21 % in HL and 9-17 % in case of ML regimes. This improvement in the frictional properties for the ECP_S3 shows that the circular textures contributes in reducing the friction in ML and HL conditions by creating the lubricant reservoirs that help in improving the lubrication at the surface interfaces. However, in case of the sample ECP_S2 there is no improvement observed in BL and ML regimes but COF reduction can be observed in HL around 1.8-4.2 %. At this regime ECP_S2 is contributing in improvement of lubrication. ECP_S1 has not shown any improvements in any lubrication regimes when compared with smooth sample. This texture pattern when closely observed is

found to have the sharp edges resulting in asperity to asperity contact that results in higher COF values.

4.2.2. COF Variation for Textured/Textured-Coated Specimens

The individual studies have been made to test the performance of the texture and coating on the smooth specimen. Synergy of these two techniques (texturing and coating) has been performed and tested on block-on-ring test. Hence, the study is made to compare the Stribeck curves of the smooth (S0), textured (ECP_S1, ECP_S2, ECP_S3) and textured-coated (ECP_S1', ECP_S2', ECP_S3') specimens. It has been already observed that the texture geometries affect positively in high sliding speeds and the coating on the surface improves the COF in the BL regimes at lower sliding speeds.

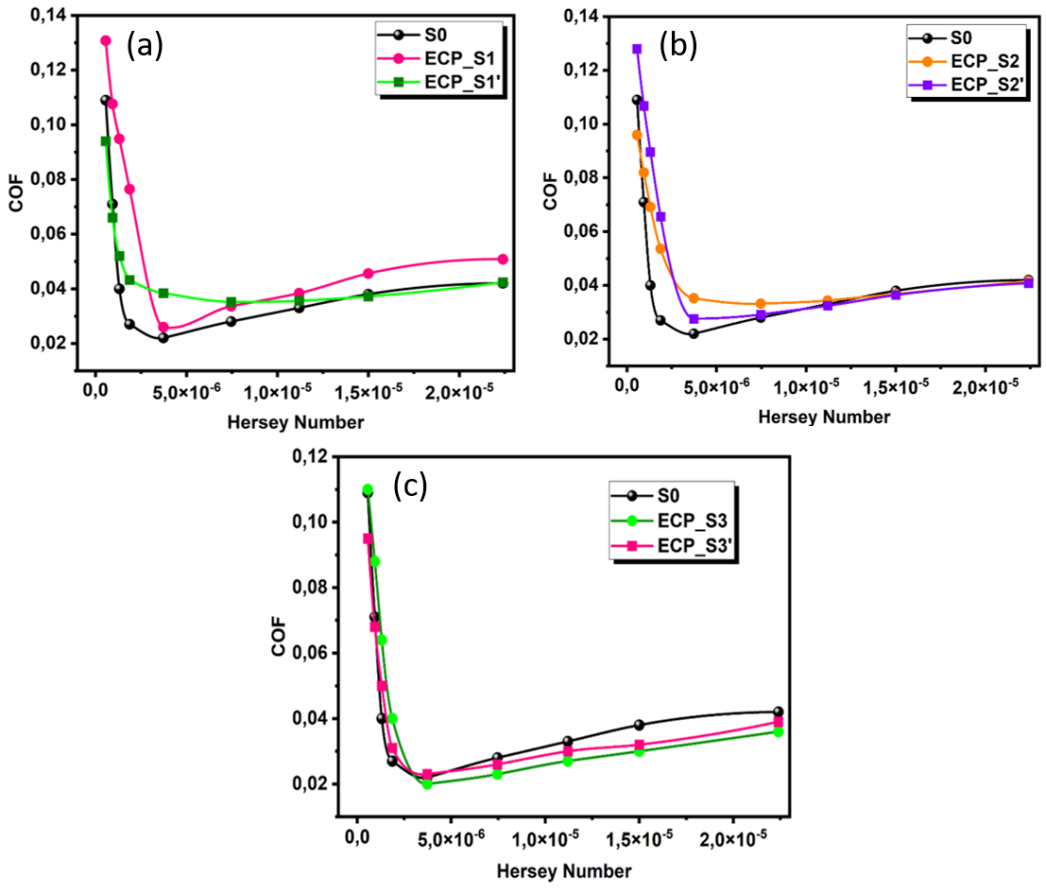

Figure 17 Stribeck curves of the (a) S0, ECP_S1 and ECP_S1' (b) S0, ECP_S2 and ECP_S2' and (c) S0, ECP_S3 and ECP_S3'

Figure 17 shows the Stribeck curves for smooth, textured and textured-coated specimens as (a) S0, ECP_S1 and ECP_S1' (b) S0, ECP_S2 and ECP_S2' and (c) S0, ECP_S3 and

ECP_S3'. It is clearly seen that the Stribeck curve of the ECP_S1' has improved after coating in comparison to the ECP_S1. The improvement is clearly seen in all the lubrication regimes however when the specimens are compared with the S0 the improvement of the COF can be found only in BL regime for ECP_S1' that is because of the solid lubrication provided by coating. The improvement of about 7 -13 % is observed at this regime for ECP_S1' and also in two sliding speeds, COF values are lower by 2.1 % at 40 rpm which is an indication of the surface property enhancement.

The Stribeck curves in Figure 17 (b) shows that ECP_S2' has lowered the COF at BL regime when compared to both the specimens S0 and ECP_S2. There is around 11.9 % of improvement of COF at 1.5rpm point in BL regime for ECP_S2' in comparison to S0, whereas in HL regime there is about 0.95 - 3.15 % of improvement. The Stribeck curve of the ECP_S2 reveals 1.8-4.2 % lower friction at HL regime as compared to S0. In case of the ECP_S2' the coating acted as the solid lubricant thereby affecting in lower COF at BL condition and HL conditions.

In Figure 17(c), the Stribeck curves of S0, ECP_S3 and ECP_S3', previously it was observed that ECP_S3 in comparison to S0 elevated the frictional properties by reducing the COF values at HL and ML regimes by 14-21 % and 9-18 %, respectively. After coating, overall improvement in the frictional properties is observed in ECP_S3' with improvement of 4.2 - 12.8% of COF in case of BL regime, 7.1%, 9.1 %, 15.8% and 7.1% at sliding speeds 20, 30, 40, 60, respectively.-15 % of improvement in ML and HL regimes in comparison to S0. This overall improvement in tribological behavior in ECP_S3' confirms the contribution of both surface modification techniques i.e. texturing and coating. The percentage improvement of all the specimens smooth, smooth-coated, textured and textured-coated is summarized in the Table 9.

Table 9 Performance of the ECP_S1, ECP_S1', ECP_S2, ECP_S2', ECP_S3 and ECP_S3' specimens in comparison to S0 in block-on-ring test

Specimens	RPM	1.5	2.5	3.5	5	10	20	30	40	60
ECP Textured & MoSeC Coated	ECP_S3'	**12.8%**	**4.2%**	-25.0%	-14.8%	-4.5%	**7.1%**	**9.1%**	**15.8%**	**7.1%**
	ECP_S2'	**11.9%**	-15.5%	-73.0%	-98.5%	-60.0%	-18.6%	-4.2%	**3.1%**	**0.9%**
	ECP_S1'	**13.8%**	**7.0%**	-30.0%	-60.0%	-74.5%	-25.7%	-7.9%	**2.1%**	-0.9%
ECP Textured	ECP_S3	-0.9%	-23.9%	-60.0%	-48.1%	**9.1%**	**17.8%**	**18.2%**	**21.0%**	**14.3%**

	ECP_S2	-17.4%	-50.4%	-124.0%	-142.9%	-25.4%	-4.3%	**1.8%**	**4.2%**	**2.8%**
	ECP_S1	-20.0%	-51.5%	-137.0%	-182.9%	-18.2%	-20.0%	-16.4%	-20.0%	-20.9%
MoSeC Coated	MoSeC_S0'	**13.3%**	**12.7%**	-1.2%	-13.3%	-6.8%	-0.5%	-0.3%	**4.7%**	**1.9%**
Smooth	S0	-	-	-	-	-	-	-	-	-

From this performance Table 9, it has been identified that the best geometric patterns out of three texture geometries is the circular dimples that shows the most improvement in frictional properties in textured as well as textured-coated specimens.

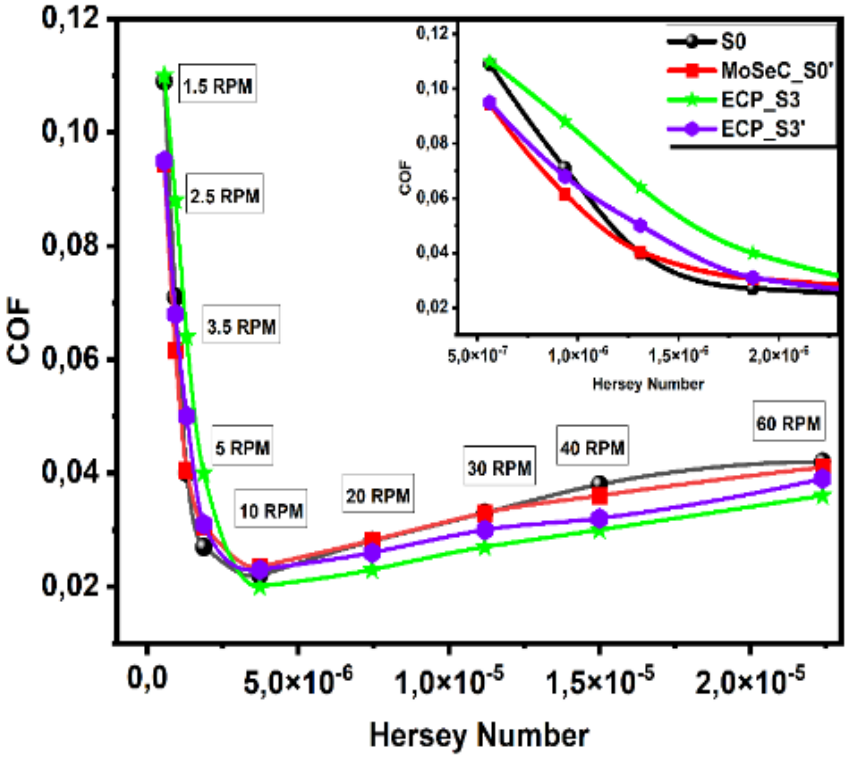

Figure 18 Stribeck curves of S0, MoSeC_S0', ECP_S3 and ECP_S3'

The circular dimple texture has shown the better performance compared to all the other geometries in ML and HL regimes, proving the textured surface retained the oil on the interface thereby providing the better lubrication properties. To make clear vision about the circular dimple textures, it is also important to compare circular textured specimens with both smooth and the smooth-coated specimens.

Figure 18, shows the Stribeck curves of the specimens S0, MoSeC_S0', ECP_S3 and ECP_S3' and it has been observed that ECP_S3' is still the best performing as compared to smooth-coated specimenMoSeC_S0' also. It can be seen clearly that the improvement of the circular textured-coated ECP_S3' specimen is very promising in all lubrication regimes in

comparison to S0 and MoSeC_S0'. This effect of texturing and coating in case of circular dimple patterns shows the synergy of texturing-coating in elevating the frictional behaviors in BL and HL regimes.

4.2.3. COF Variation of Dual Textured and Coated Specimens:

As circular textured specimen shows the best performance, therefore dual texturing technique has been applied to obtain circular dimples. Figure 19 depicts the Stribeck curves for smooth (S0), smooth-coated with WSC as well as MoSeC (WSC_S0', MoSeC_S0'), dual textured (EDM_ECP_S3) and dual-textured-coated with WSC as well as MoSeC (EDM_ECP_MoSeC_S3' and EDM_ECP_WSC_S3') specimens.

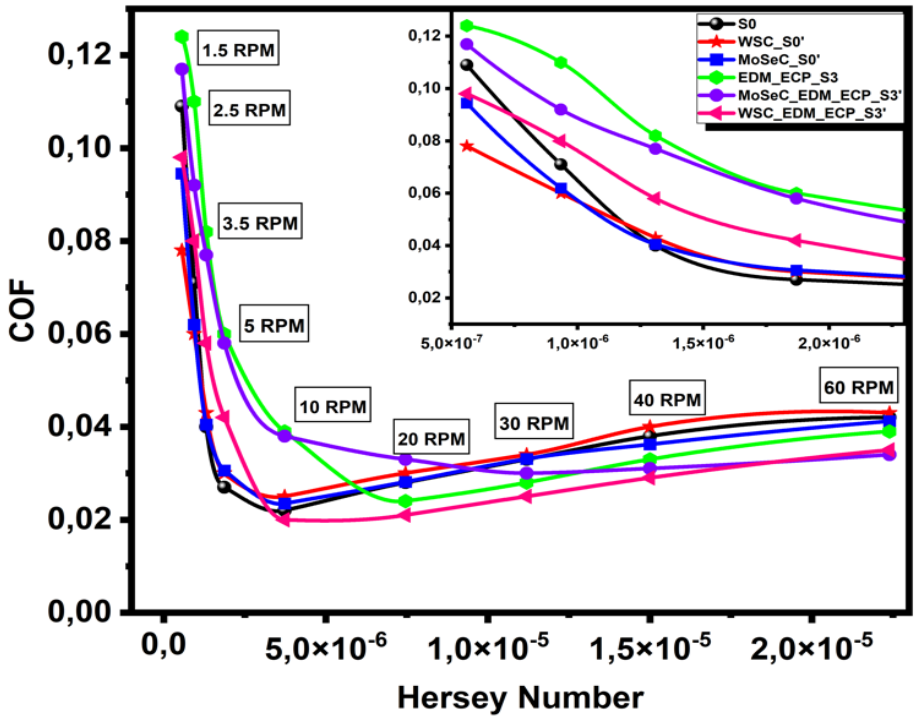

Figure 19 Stribeck curves of the S0, MoSeC_S0', WSC_S0',EDM_ECP_MoSeC_S3 and EDM_ECP_WSC_S3'

The specimens exhibit the improvement in the frictional behavior in comparison to the smooth sample. Among all these specimens, EDM_ECP_MoSeC_S3' shows an improvement of 0.91% in BL regime and 9-19% in HL regime, whereas EDM_ECP_WSC_S3' shows 10% improvement in BL and around 9-25 % and 16-24 % in ML and HL regimes, respectively. These improvements in case of the dual textured and

coated specimens are the synergistic effects of the surface coating enhancing frictional properties in BL regime and surface texturing in ML and HL regimes. The performance improvements in the dual textured specimens in comparison to the smooth and smooth-coated specimens are summarized in the Table 10.

Table 10 Performance of the MoSeC_S0', WSC_S0', EDM_ECP_MoSeC_S3 and EDM_ECP_WSC_S3' to S0

RPM	1.5	2.5	3.5	5	10	20	30	40	60
EDM_ECP_WSC_S3'	**10.1%**	-12.7%	-45.0%	-55.5%	**9.1%**	**25.0%**	**24.3%**	**23.7%**	**16.7%**
EDM_ECP_MoSeC_S3'	**0.9%**	-29.6%	-92.5%	-114.8%	-40.9%	-7.1%	**9.1%**	**18.4%**	**19.0%**
EDM_ECP_S3	**7.1%**	**13.1%**	**15.1%**	**14.3%**	-77.3%	-122.2%	-105.0%	-54.9%	-13.8%
MoSeC_S0'	**13.3%**	**12.7%**	-1.3%	-13.3%	-6.8%	-0.5%	-0.3%	**4.7%**	**1.9%**
WSC_S0'	**35.8%**	**15.5%**	-7.5%	-11.1%	-13.7%	-7.1%	-3.0%	-5.3%	-2.4%
S0	--	--	--	--	--	--	--	--	--

4.3. Surface Morphology

During the block-on-ring experiment, there is contact take place between the specimen and the counter body (ring) that makes the wear scratch on the specimen. Hence, to analyze this material disintegration during the test, surface of the specimens has been analyzed with SEM. However, in this study there is no prominent wear scratch has been observed because the number of cycles of test at different sliding speeds and the load applied were not enough to create the wear scratch. Still there was an interaction between the two material surfaces (specimen & ring) so it is important to study the surface morphology. This will be helpful for understanding the variations in the tribological behaviors observed with texturing and coating.

4.3.1. Wear Scratch on ECP_S3 & ECP_S3'

The surface of the sample ECP_S3 was analyzed after the sliding test, it was found that there was no wear scratch on the textured surface and however there were traces of the mild scratches which were observed. Figure - 20(A) shows the textured surface on ECP_S3 and (B) shows the scratch on the surface of the sample and (C) shows the scratch at the texture boundaries. It is observed that the boundaries of the textures are smooth and the interaction created the storage area for the lubricant and allowed the easy flow which resulted in reducing the friction in ML and BL regimes.

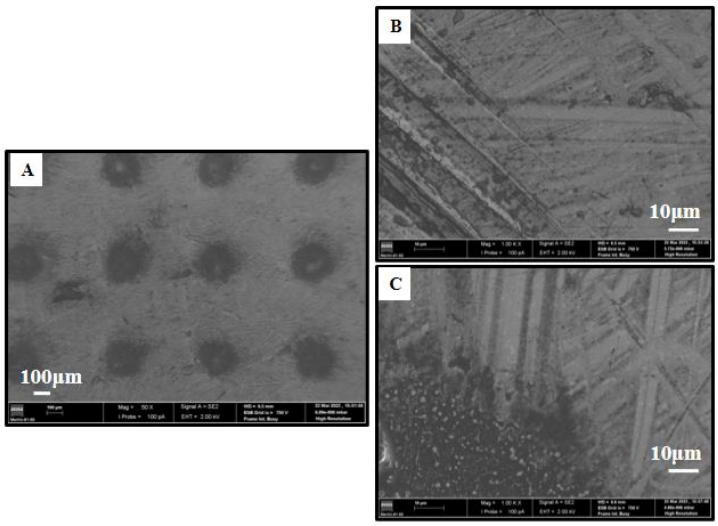

Figure 20 SEM images of ECP_ S3 specimen(A) texturedsurface (B) Scratch on the surface and (C) scratchat the boundary of the texture

The surface of the coated specimenECP_S3' after sliding test is also analyzed. There is still no significant wear on the surface and only the traces of scratch were identified that is shown in the Figure 21(A) and the scratch is magnified to see the disintegration of the coated surface.

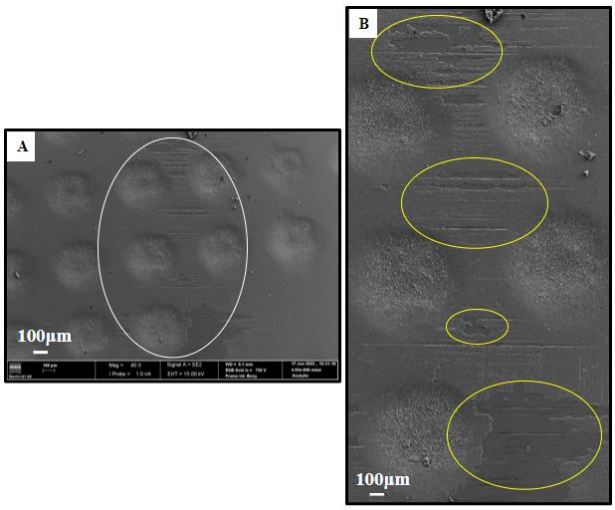

Figure 21 SEM image of the ECP_S3' sample (A) texture surface (B) magnifiedimage of the scratch on the surface

In figure 21(B), the marked regions represent the disintegration of the MoSeC coating during the sliding test; it is an indication of the solid lubricant nature of the coating that has influenced the frictional properties. The reduction in the COF at the BL regime was the result

of these disintegrations of MoSeC coating that acted as the sacrificial layer preventing in the higher friction rate.

4.3.2. EDS Analysis on Coatings

The chemical composition of the coated surface was analyzed using EDS to check if the surfaces of the specimens were uniformly coated. Figure 22, (A) shows the surface of the sample MoSeC_S0' and (B) shows the EDS data of the selected region. It is clearly seen from the data that the atomic weight % of the Se is around 51.5%, with Mo and C around 29.2% and 16.9% respectively. There are also traces of Fe with 1.3% due to the material composition and Ar of 0.4% due to the deposition medium. However, it can be concluded that the coating was uniformly distributed on the surface constituting around 97.6% of the surface.

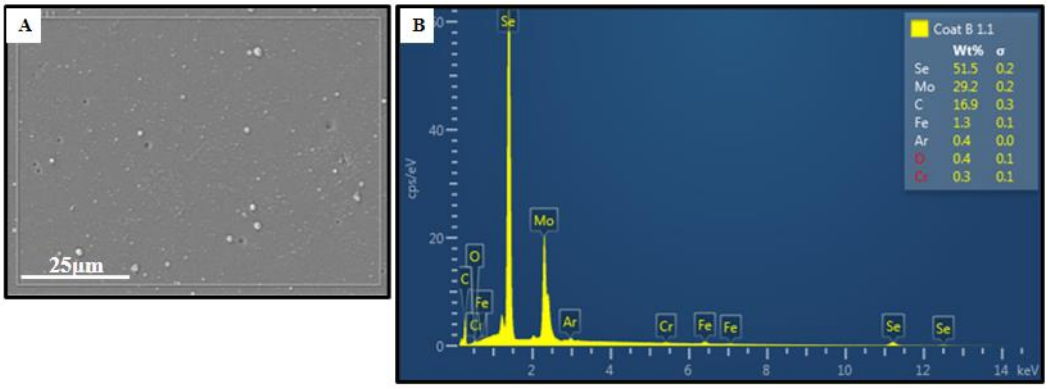

Figure 22 SEM image of the MoSeC_S0' sample (A) sample surface (B) EDS data of the surface

EDS was also performed on the sample WSC_S0' and its chemical composition was identified to check the uniformity of the distribution of the coating on the surface. Figure 23 (A) shows the SEM image of the sample WSC_S0' and (B) EDS data. The atomic weight % of the W is found to be about 63.0% along with C and S about 16.9% and 16.8% respectively with the traces of Fe 1.4 %. The data confirms the uniform distribution of the WSC coating on the surface.

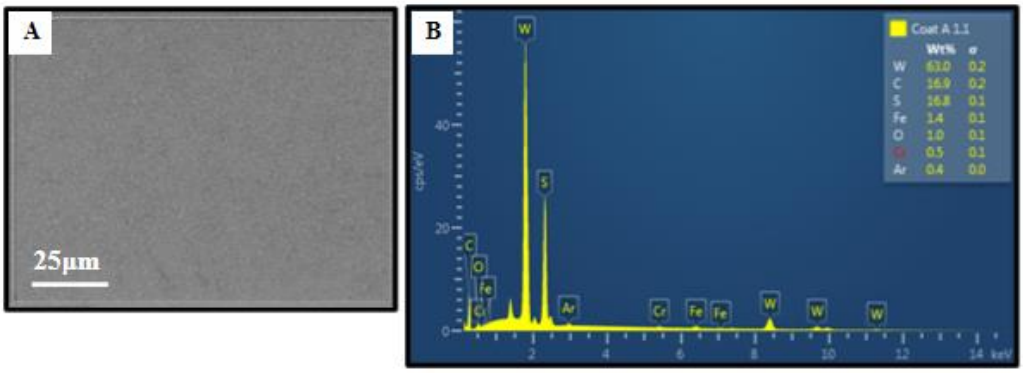

Figure 23 SEM image of the WSC_S0' sample (A) sample surface (B) EDS data of the surface

4.3.3. EDS Analysis on ECP_S3 & ECP_S3'

EDS analysis was performed at the surrounding boundaries of the textures on the sample ECP_S3, Figure 24 (A), shows the textured surface of the ECP_S1, (B) shows the magnified region of the texture boundary along with (C) showing the EDS data of the chemical composition at that region. It is important to understand the reasons for the lower frictional behaviors of the circular textures in ECP_S3 at ML and BL regimes. The smooth surface that has resulted from the material disintegration at the edges of the dimples is one of the reasons and it was formed due to the traces of the metallic debris which was identified to be Fe with 61.8%. Further these regions have contributed in storing the lubricant providing better lubrication at the ML and BL regimes enhancing the frictional properties.

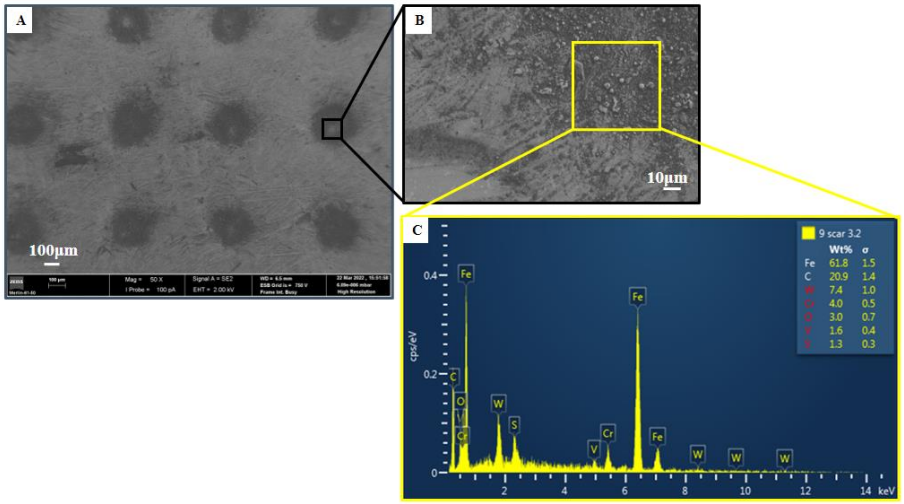

Figure 24 SEM image of S3 sample (A) image of surface texture (B) magnified image of dimple surface (C) EDS data of the magnified image

The EDS data of the dimple surface of ECP_S3' was analyzed to check the traces of the metal that is contributing in the solid lubrication in the coated region which resulted in reducing the COF values at the BL regime. Figure 25 (A), shows the textured surface of the ECP_S3', (B) shows the magnified dimple surface and (C) shows the EDS data at the magnified surface. It was observed that similar wt % of the metals were present at the surface interface that was identified for ECP_MoSeC_S0' sample, however this coating has provided an significant amount of solid lubricants at the BL regime where the material surface interface experiences body-body contact with fewer lubricant.

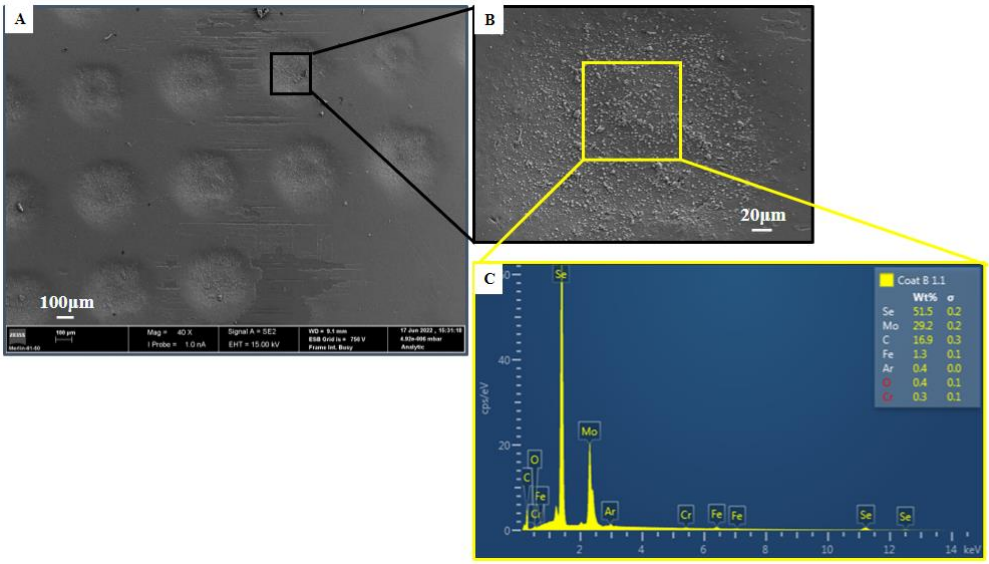

Figure 25 SEM image of S3' sample (A) image of surface texture (B) magnified image of dimple surface (C) EDS data of the magnified image

CHAPTER 5

5. CONCLUSION AND RECOMMENDATIONS

The study is focused on determining the synergistic effects of the texture-coating combination on the friction behaviours of the material surface. There are various aspects that were considered in this study to bring the contribution of techniques used in day to day applications in case of piston/cylinder materials. This combinational study featuring the two surface modification techniques are very essential for enhancing the fuel efficiency of the internal combustion engines.

The two techniques involved in this investigation were ECP and dual texturing techniques with TMD coatings of MoSeC and WSC films. The studies were conducted both individually as well as comparatively on the material samples to bring the coordination in the results in terms of reliability. There were also studies based on varying the texture geometries in the ECP technique to understand the role of dimple geometries in effecting the tribological behaviours. The best performing geometry was used to replicate by dual texturing (EDM+ECP) technique to understand the performance by dual texturing techniques. Further, these textured samples were coated with MoSeC and WSC films and were tested to compare the synergistic effects of texturing and coating on the frictional characteristics.

The block-on-ring experiment used in this study plays a significant role in determining the COF values of the samples when compared to the other tribometer experiments because of its advantage for testing under uniform Hertzian contacts at the interface. Another important factor that has to be considered in this study is the usage of non-additive lubricant for experiments, the improvements in COF with this lubricant is significantly predominant for the studies conducted with lubricants without additives.

5.1. Important Points

There are several conclusions that can be drawn from this study focusing on the investigation of the tribological behaviour of the textured steel coated with TMD films; they are:

a) The geometry of the dimples in the surface texturing process plays an important role in affecting the frictional properties of the materials, in this study out of three geometric patterns circular dimples showed the significant effects on improving the tribological behaviours by reducing the COF values at ML and BL regimes.
b) The MoSeC and WSC coatings helped in improving the lubrication properties of the material surface at the BL regime, it showed a lower COF values at this regime by acting as a solid lubricant in comparison to the smooth sample.
c) The comparative study of the uncoated-textured and coated-textured samples revealed that the roles of coating and texturing is improving the frictional properties in respective lubrication regimes; i.e., texturing is affecting in ML and HL regimes and coating in BL regimes.
d) The samples with circular dimples with and without coating showed the betterment in the tribological properties in comparison to the smooth samples thereby exhibiting as the significant texture geometry for the surface enhancement processes in piston/cylinder applications.
e) The dual texturing method along with the surface coating has shown the improvement in the tribological properties of the smooth sample in all the lubrication regimes in both coated and non-coated conditions.

5.2. Scope of future work

For future work, it is recommended to study the same effects based on different lubricants with additives, by changing temperatures of the additives and also by increasing the load with rotational speed to analyze the wear behaviours on the surface. Changing these parameters and verifying the results would significantly help the industries in selecting the desirable techniques for the materials used in piston/cylinder applications.

6. REFERENCES

[1] Mourier, L., Mazuyer, D., Ninove, F.P. and Lubrecht, A.A., 2010. Lubrication mechanisms with laser-surface-textured surfaces in elastohydrodynamic regime. Proceedings of the Institution of Mechanical Engineers, Part J: Journal of Engineering Tribology, 224(8), pp.697-711.

[2] Etsion, I. and Halperin, G., 2002. A laser surface textured hydrostatic mechanical seal. *Tribology Transactions*, *45*(3), pp.430-434.

[3] Etsion, I., Kligerman, Y. and Halperin, G., 1999. Analytical and experimental investigation of laser-textured mechanical seal faces. *Tribology Transactions*, *42*(3), pp.511-516.

[4] Etsion, I., 2005. State of the art in laser surface texturing. *J. Trib.*, *127*(1), pp.248-253.

[5] Tomanik, E., Profito, F.J. and Zachariadis, D.C., 2013. Modelling the hydrodynamic support of cylinder bore and piston rings with laser textured surfaces. *Tribology international*, *59*, pp.90-96.

[6] Arumugaprabu, V., Ko, T.J., Kumaran, T., Kurniawan, R. and Uthayakumar, M., 2018. A brief review on importance of surface texturing in materials to improve the tribological performance. *Reviews on Advanced Materials Science*, *53*(1), pp.40-48.

[7] Gadeschi, G.B., Backhaus, K. and Knoll, G., 2012. Numerical analysis of laser-textured piston-rings in the hydrodynamic lubrication regime. *Journal of Tribology*, *134*(4).

[8] Kawasegi, N., Sugimori, H., Morimoto, H., Morita, N. and Hori, I., 2009. Development of cutting tools with microscale and nanoscale textures to improve frictional behavior. *Precision Engineering*, *33*(3), pp.248-254.] .

[9] Wan, Y. and Xiong, D.S., 2008. The effect of laser surface texturing on frictional performance of face seal. *Journal of materials processing technology*, *197*(1-3), pp.96-100.

[10] Etsion, I. and Sher, E., 2009. Improving fuel efficiency with laser surface textured piston rings. *Tribology International*, *42*(4), pp.542-547.

[11] Qiu, M., Bailey, B.N., Stoll, R. and Raeymaekers, B., 2014. The accuracy of the compressible Reynolds equation for predicting the local pressure in gas-lubricated textured parallel slider bearings. *Tribology international*, *72*, pp.83-89.

[12] Chyr, A., Qiu, M., Speltz, J.W., Jacobsen, R.L., Sanders, A.P. and Raeymaekers, B., 2014. A patterned microtexture to reduce friction and increase longevity of prosthetic hip joints. *Wear*, *315*(1-2), pp.51-57.

[13] Quazi, M.M., Fazal, M.A., Haseeb, A.S.M.A., Yusof, F., Masjuki, H.H. and Arslan, A., 2016. Laser-based surface modifications of aluminum and its alloys. *Critical Reviews in Solid State and Materials Sciences*, *41*(2), pp.106-131.

[14] Fotovvati, B., Namdari, N. and Dehghanghadikolaei, A., 2019. On coating techniques for surface protection: A review. *Journal of Manufacturing and Materials Processing*, *3*(1), p.28.

[15] Moghaddam, P.V., Prakash, B., Vuorinen, E., Fallqvist, M., Andersson, J.M. and Hardell, J., 2021. High temperature tribology of TiAlN PVD coating sliding against 316L stainless steel and carbide-free bainitic steel. *Tribology International*, *159*, p.106847.

[16] Bhushan, B. and Gupta, B.K., 1991. Handbook of tribology: materials, coatings, and surface

[17] Hamilton, D.B., Walowit, J.A. and Allen, C.M., 1966. A theory of lubrication by microirregularities.

[18] Gachot, C., Rosenkranz, A., Hsu, S.M. and Costa, H.L., 2017. A critical assessment of surface texturing for friction and wear improvement. *Wear*, *372*, pp.21-41.

[19] Jen, T.C., Tuchowski, F. and Chen, Y.M., 2005, January. Investigation of thermosyphon cooling for drilling operation: an experimental study. In *ASME International Mechanical Engineering Congress and Exposition* (Vol. 42231, pp. 59-67). [20] Chiou, R.Y., Aynbinder, V., Stepanskiy, L.G., Lu, L., Rauniar, S., Chen, J.S. and North, M.T., 2005, January. Analytical study of the effect of heat pipe cooling in machining. In *ASME International Mechanical Engineering Congress and Exposition* (Vol. 42231, pp. 13-21).

[21] Patel, D., Jain, V.K. and Ramkumar, J., 2018. Micro texturing on metallic surfaces: State of the art. *Proceedings of the Institution of Mechanical Engineers, Part B: Journal of Engineering Manufacture*, *232*(6), pp.941-964.

[22] Bechert, D.W., Bruse, M. and Hage, W., 2000. Experiments with three-dimensional riblets as an idealized model of shark skin. *Experiments in fluids*, *28*(5), pp.403-412.]

[23] Bhushan, B., 2009. Biomimetics: lessons from nature–an overview. *Philosophical Transactions of the Royal Society A: Mathematical, Physical and Engineering Sciences*, *367*(1893), pp.1445-1486.

[24] Ponsonnet, L., Reybier, K., Jaffrezic, N., Comte, V., Lagneau, C., Lissac, M. and Martelet, C., 2003. Relationship between surface properties (roughness, wettability) of titanium and titanium alloys and cell behaviour. *Materials Science and Engineering: C*, *23*(4), pp.551-560.

[25] Etsion, I. and Sher, E., 2009. Improving fuel efficiency with laser surface textured piston rings. *Tribology International*, *42*(4), pp.542-547.

[26] Ball, P., 1999. Engineering shark skin and other solutions. *Nature*, *400*(6744), pp.507-509.

[27] Kim, B.H., Na, C.W., Lee, Y.S., Choi, D.K. and Chu, C.N., 2005. Micro electrochemical machining of 3D micro structure using dilute sulfuric acid. *CIRP annals*, *54*(1), pp.191-194.

[28] Datta, M., 1995. Fabrication of an array of precision nozzles by through-mask electrochemical micromachining. *Journal of the Electrochemical Society*, *142*(11), p.3801.

[29] Bhattacharyya, B., Munda, J. and Malapati, M., 2004. Advancement in electrochemical micro-machining. *International Journal of Machine Tools and Manufacture*, *44*(15), pp.1577-1589.

[30] Vranceanu, D.M., Ionescu, I.C., Ungureanu, E., Cojocaru, M.O., Vladescu, A. and Cotrut, C.M., 2020. Magnesium doped hydroxyapatite-based coatings obtained by pulsed galvanostatic electrochemical deposition with adjustable electrochemical behavior. *Coatings*, *10*(8), p.727.

[31] Chen, X., Qu, N., Hou, Z., Wang, X. and Zhu, D., 2017. Friction reduction of chrome-coated surface with micro-dimple arrays generated by electrochemical micromachining. *Journal of Materials Engineering and Performance*, *26*(2), pp.667-675.

[32] Byun, J.W., Shin, H.S., Kwon, M.H., Kim, B.H. and Chu, C.N., 2010. Surface texturing by micro ECM for friction reduction. *International Journal of Precision Engineering and Manufacturing*, *11*(5), pp.747-753.

[33] Mishra, S.P. and Polycarpou, A.A., 2011. Tribological studies of unpolished laser surface textures under starved lubrication conditions for use in air-conditioning and refrigeration compressors. *Tribology International*, *44*(12), pp.1890-1901.

[34] Byun, J.W., Shin, H.S., Kwon, M.H., Kim, B.H. and Chu, C.N., 2010. Surface texturing by micro ECM for friction reduction. *International Journal of Precision Engineering and Manufacturing*, *11*(5), pp.747-753.

[35] Zeng, Z., Wang, Y., Wang, Z., Shan, D. and He, X., 2012. A study of micro-EDM and micro-ECM combined milling for 3D metallic micro-structures. *Precision Engineering*, *36*(3), pp.500-509.

[36] Masuzawa, T., 2000. State of the art of micromachining. *Cirp Annals*, *49*(2), pp.473-488.

[37]Coblas, D.G., Fatu, A., Maoui, A. and Hajjam, M., 2015. Manufacturing textured surfaces: State of art and recent developments. *Proceedings of the institution of mechanical engineers, Part J: Journal of Engineering Tribology*, *229*(1), pp.3-29.

[38] Lauwers, B., Kruth, J.P., Liu, W., Eeraerts, W., Schacht, B. and Bleys, P., 2004. Investigation of material removal mechanisms in EDM of composite ceramic materials. *Journal of Materials Processing Technology*, *149*(1-3), pp.347-352.

[39] Uhlmann, E., Piltz, S. and Doll, U., 2005. Machining of micro/miniature dies and moulds by electrical discharge machining—recent development. *Journal of Materials Processing Technology*, *167*(2-3), pp.488-493.

[40] Algodi, S.J., Murray, J.W., Fay, M.W., Clare, A.T. and Brown, P.D., 2016. Electrical discharge coating of nanostructured TiC-Fe cermets on 304 stainless steel. *Surface and Coatings Technology*, *307*, pp.639-649.

[41] Koshy, P. and Tovey, J., 2011. Performance of electrical discharge textured cutting tools. *CIRP annals*, *60*(1), pp.153-156.

[42] Kim, D.M., Lee, I., Kim, S.K., Kim, B.H. and Park, H.W., 2016. Influence of a micropatterned insert on characteristics of the tool–workpiece interface in a hard turning process. *Journal of Materials Processing Technology*, *229*, pp.160-171.

[43] Zavos, A. and Nikolakopoulos, P.G., 2015. Tribological characterization of smooth and artificially textured coated surfaces using block-on-ring tests. *FME Transactions*, *43*(3), pp.191-197.

[44] Gachot, C., Rosenkranz, A., Hsu, S.M. and Costa, H.L., 2017. A critical assessment of surface texturing for friction and wear improvement. *Wear*, *372*, pp.21-41.

[45] Zhan, X., Yi, P., Liu, Y., Xiao, P., Zhu, X. and Ma, J., 2020. Effects of single-and multi-shape laser-textured surfaces on tribological properties under dry friction. *Proceedings of the Institution of Mechanical Engineers, Part C: Journal of Mechanical Engineering Science*, *234*(7), pp.1382-1392.

[46] Grützmacher, P.G., Rosenkranz, A., Szurdak, A., König, F., Jacobs, G., Hirt, G. and Mücklich, F., 2018. From lab to application-improved frictional performance of journal bearings induced by single-and multi-scale surface patterns. *Tribology International*, *127*, pp.500-508.

[47] Ogawa, H., Sasaki, S., Korenaga, A., Miyake, K., Nakano, M. and Murakami, T., 2010. Effects of surface texture size on the tribological properties of slideways. *Proceedings of the Institution of Mechanical Engineers, Part J: Journal of Engineering Tribology*, *224*(9), pp.885-890.

[48] Ogawa, H., Sasaki, S., Korenaga, A., Miyake, K., Nakano, M. and Murakami, T., 2010. Effects of surface texture size on the tribological properties of slideways. *Proceedings of the Institution of Mechanical Engineers, Part J: Journal of Engineering Tribology*, *224*(9), pp.885-890.

[49] Sun, Q., Hu, T., Fan, H., Zhang, Y. and Hu, L., 2015. Dry sliding wear behavior of TC11 alloy at 500° C: influence of laser surface texturing. *Tribology International*, *92*, pp.136-145.

[50] Xing, Y., Deng, J., Feng, X. and Yu, S., 2013. Effect of laser surface texturing on Si3N4/TiC ceramic sliding against steel under dry friction. *Materials & Design (1980-2015)*, *52*, pp.234-245.

[51] Rosenkranz, A., Reinert, L., Gachot, C. and Mücklich, F., 2014. Alignment and wear debris effects between laser-patterned steel surfaces under dry sliding conditions. *Wear*, *318*(1-2), pp.49-61.

[52] Rosenkranz, A., Reinert, L., Gachot, C., Aboufadl, H., Grandthyll, S., Jacobs, K., Müller, F. and Mücklich, F., 2015. Oxide formation, morphology, and nanohardness of laser-patterned steel surfaces. *Advanced Engineering Materials*, *17*(8), pp.1234-1242.

[53] Li, J., Liu, S., Yu, A. and Xiang, S., 2018. Effect of laser surface texture on CuSn6 bronze sliding against PTFE material under dry friction. *Tribology International*, *118*, pp.37-45.

[54] Hamilton, D.B., Walowit, J.A. and Allen, C.M., 1966. A theory of lubrication by microirregularities.

[55] Ronen, A., Etsion, I. and Kligerman, Y., 2001. Friction-reducing surface-texturing in reciprocating automotive components. *Tribology transactions*, *44*(3), pp.359-366.

[56] Hansen, J., Björling, M. and Larsson, R., 2019. Mapping of the lubrication regimes in rough surface EHL contacts. *Tribology International*, *131*, pp.637-651.

[57] Kovalchenko, A., Ajayi, O., Erdemir, A., Fenske, G. and Etsion, I., 2004. The effect of laser texturing of steel surfaces and speed-load parameters on the transition of lubrication regime from boundary to hydrodynamic. *Tribology Transactions*, *47*(2), pp.299-307.

[58] Amanov, A., Cho, I.S., Pyoun, Y.S., Lee, C.S. and Park, I.G., 2012. Micro-dimpled surface by ultrasonic nanocrystal surface modification and its tribological effects. *Wear*, *286*, pp.136-144.

[59] Rapoport, L., Moshkovich, A., Perfilyev, V., Lapsker, I., Halperin, G., Itovich, Y. and Etsion, I., 2008. Friction and wear of MoS2 films on laser textured steel surfaces. *Surface and Coatings Technology*, *202*(14), pp.3332-3340.

[60] Braun, D., Greiner, C., Schneider, J. and Gumbsch, P., 2014. Efficiency of laser surface texturing in the reduction of friction under mixed lubrication. *Tribology international*, *77*, pp.142-147.

[61] Zavos, A. and Nikolakopoulos, P.G., 2015. Tribological characterization of smooth and artificially textured coated surfaces using block-on-ring tests. *FME Transactions*, *43*(3), pp.191-197.

[62] Andersson, P., Koskinen, J., Varjus, S.E., Gerbig, Y., Haefke, H., Georgiou, S., Zhmud, B. and Buss, W., 2007. Microlubrication effect by laser-textured steel surfaces. *Wear*, *262*(3-4), pp.369-379.

[63] Borghi, A., Gualtieri, E., Marchetto, D., Moretti, L. and Valeri, S., 2008. Tribological effects of surface texturing on nitriding steel for high-performance engine applications. *Wear*, *265*(7-8), pp.1046-1051.

[64] Xing, Y., Deng, J., Feng, X. and Yu, S., 2013. Effect of laser surface texturing on Si3N4/TiC ceramic sliding against steel under dry friction. *Materials & Design (1980-2015)*, *52*, pp.234-245.

[65] Wang, Z., Zhao, Q., Wang, C. and Zhang, Y., 2015. Modulation of dry tribological property of stainless steel by femtosecond laser surface texturing. *Applied Physics A*, *119*(3), pp.1155-1163.

[66] Kang, M., Park, Y.M., Kim, B.H. and Seo, Y.H., 2015. Micro-and nanoscale surface texturing effects on surface friction. *Applied Surface Science*, *345*, pp.344-348.

[67] Berghaus, B., 1938. Improvements in and Related to the Coating of Articles by Means of Thermally Vapourized Material. *UK Patent*, *510992*.

[68] Mattox, D.M., 1998. Handbook of Physical Vapor Deposition (PVD) Processing, Film Formation, Adhesion, Surface Preparation and Contamination Control, 1998. *Dostupné z: http://lib. semi. ac. cn*, *8080*.

[69] Hoche, H., Groß, S. and Oechsner, M., 2014. Development of new PVD coatings for magnesium alloys with improved corrosion properties. *Surface and Coatings Technology*, *259*, pp.102-108.

[70] Skordaris, G., Bouzakis, K.D., Kotsanis, T., Charalampous, P., Bouzakis, E., Lemmer, O. and Bolz, S., 2016. Film thickness effect on mechanical properties and milling performance of nano-structured multilayer PVD coated tools. *Surface and Coatings Technology*, *307*, pp.452-460.

[71] Jen, Y.J., Lakhtakia, A., Yu, C.W. and Lin, C.T., 2009. Vapor-deposited thin films with negative real refractive index in the visible regime. *Optics express*, *17*(10), pp.7784-7789.

[72] Baptista, A., Silva, F., Porteiro, J., Míguez, J. and Pinto, G., 2018. Sputtering physical vapour deposition (PVD) coatings: A critical review on process improvement and market trend demands. *Coatings*, *8*(11), p.402.

[73] Kelly, P.J. and Arnell, R.D., 2000. Magnetron sputtering: a review of recent developments and applications. *Vacuum*, *56*(3), pp.159-172.

[74] Joshi, P., Gesawat, A.A. and Singh, K., 2015. Development and characterization of Ti-Nb-N coatings on stainless steel using reactive DC magnetron sputtering. *ChemSci Rev Lett*, *4*(16), pp.1059-1068.

[75] Stachowiak, G.W. and Batchelor, A.W., 2013. *Engineering tribology*. Butterworth-heinemann.

[76] Aouadi, S.M., Luster, B., Kohli, P., Muratore, C. and Voevodin, A.A., 2009. Progress in the development of adaptive nitride-based coatings for high temperature tribological applications. *Surface and Coatings Technology*, *204*(6-7), pp.962-968.

[77] Polcar, T. and Cavaleiro, A., 2011. Self-adaptive low friction coatings based on transition metal dichalcogenides. *Thin Solid Films*, *519*(12), pp.4037-4044.

[78] Donnet, C. and Erdemir, A., 2004. Historical developments and new trends in tribological and solid lubricant coatings. *Surface and coatings technology*, *180*, pp.76-84.

[79] Gustavsson, F. and Jacobson, S.J.T.I., 2016. Diverse mechanisms of friction induced self-organisation into a low-friction material–An overview of WS2 tribofilm formation. *Tribology International*, *101*, pp.340-347.

[80] Polcar, T., Gustavsson, F., Thersleff, T., Jacobson, S. and Cavaleiro, A., 2012. Complex frictional analysis of self-lubricant WSC/Cr coating. *Faraday Discussions*, *156*(1), pp.383-401.

[81] Yaqub, T.B., Vuchkov, T., Evaristo, M. and Cavaleiro, A., 2019. DCMS Mo-Se-C solid lubricant coatings–Synthesis, structural, mechanical and tribological property investigation. *Surface and Coatings Technology*, *378*, p.124992.

[82] Guo, Y., Tan, H., Cao, Z., Wang, D. and Zhang, S., 2018. Mechanical and Unlubricated Sliding Wear Properties of Nitrile Rubber Reinforced with Micro Glass Flake. *Polymers*, *10*(7), p.705.

[83] Mitsoulis, E., Battisti, M., Neunhäuserer, A., Perko, L., Friesenbichler, W., Ansari, M. and Hatzikiriakos, S.G., 2017. Flow behaviour of rubber in capillary and injection moulding dies. *Plastics, Rubber and Composites*, *46*(3), pp.110-118.

[84] Leyland, A. and Matthews, A., 2000. On the significance of the H/E ratio in wear control: a nanocomposite coating approach to optimised tribological behaviour. *Wear*, *246*(1-2), pp.1-11.

[85] Caessa, J., Vuchkov, T., Yaqub, T.B. and Cavaleiro, A., 2021. On the Microstructural, Mechanical and Tribological Properties of Mo-Se-C Coatings and Their Potential for Friction Reduction against Rubber. *Materials*, *14*(6), p.1336.

[86] Prasad, S. and Zabinski, J., 1997. Super slippery solids. *Nature*, *387*(6635), pp.761-763.

[87] Vazirisereshk, M.R., Martini, A., Strubbe, D.A. and Baykara, M.Z., 2019. Solid lubrication with MoS2: a review. *Lubricants*, *7*(7), p.57.

[88] Rigato, V., Maggioni, G., Boscarino, D., Sangaletti, L., Depero, L., Fox, V.C., Teer, D. and Santini, C., 1999. A study of the structural and mechanical properties of Ti= MoS2 coatings deposited by closed field unbalanced magnetron sputter ion plating. *Surface and Coatings Technology*, *116*, pp.176-183.

[89] Singh, H., Mutyala, K.C., Mohseni, H., Scharf, T.W., Evans, R.D. and Doll, G.L., 2015. Tribological performance and coating characteristics of sputter-deposited Ti-doped MoS2 in rolling and sliding contact. *Tribology Transactions*, *58*(5), pp.767-777.

[90] Scharf, T.W., Rajendran, A., Banerjee, R. and Sequeda, F., 2009. Growth, structure and friction behavior of titanium doped tungsten disulphide (Ti-WS2) nanocomposite thin films. *Thin Solid Films*, *517*(19), pp.5666-5675.

[91] Vuchkov, T., Evaristo, M., Yaqub, T.B. and Cavaleiro, A., 2020. The effect of substrate location on the composition, microstructure and mechano-tribological properties of WSC coatings deposited by magnetron sputtering. *Surface and Coatings Technology*, *386*, p.125481.

[92] Amanov, A., Watabe, T., Tsuboi, R. and Sasaki, S., 2013. Improvement in the tribological characteristics of Si-DLC coating by laser surface texturing under oil-lubricated point contacts at various temperatures. *Surface and Coatings Technology*, *232*, pp.549-560.

[93] Meng, R., Deng, J., Liu, Y., Duan, R. and Zhang, G., 2018. Improving tribological performance of cemented carbides by combining laser surface texturing and WSC solid lubricant coating. *International Journal of Refractory Metals and Hard Materials*, *72*, pp.163-171.

[94] Wu, Z., Xing, Y., Huang, P. and Liu, L., 2017. Tribological properties of dimple-textured titanium alloys under dry sliding contact. *Surface and Coatings Technology*, *309*, pp.21-28.

[95] Oksanen, J., Hakala, T.J., Tervakangas, S., Laakso, P., Kilpi, L., Ronkainen, H. and Koskinen, J., 2014. Tribological properties of laser-textured and ta-C coated surfaces with burnished WS2 at elevated temperatures. *Tribology International*, *70*, pp.94-103.

[96] Basnyat, P., Luster, B., Muratore, C., Voevodin, A.A., Haasch, R., Zakeri, R., Kohli, P. and Aouadi, S.M., 2008. Surface texturing for adaptive solid lubrication. *Surface and Coatings Technology*, *203*(1-2), pp.73-79.

[97] Doll, N.P., 2015. *Modeling thermomechanical behavior of polymer gears* (Doctoral dissertation, University of Wisconsin--Madison).